AN ABSTRACT OF THE THESIS OF

FRANKLIN BARRERO-QUIROGA (Name) for the MASTER OF SCIENCE (Degree)

in CIVIL ENGINEERING (Major) presented on April 1, 1974 (Date)

Title: PILE HAMMER SELECTION BY DRIVING STRESS ANALYSIS

Abstract approved: Redacted for privacy

Thomas J. McClellan

Redacted for privacy

Warren L. Schroeder

This paper presents an application of the wave equation to the problem of selecting a driving hammer for prestressed concrete piles. The potentially damaging effects of these types of hammers on various prestressed concrete piles were analyzed by means of parametric studies carried out on a hypothetical group of problems and two case histories. A computer program written by T. C. Edwards and largely based on the work of E. A. L. Smith was used to analyze the driving stresses produced in the pile by driving it with steam-air hammers.

For each hammer the variation of driving stresses in the pile due to variations of cushion characteristics, soil resistance, depth of embedment, length of pile and variations in the soil properties was studied.

Throughout the study it was seen that the tensile stresses produced by a single acting hammer were much higher than corresponding

stresses produced by a double acting hammer of the same energy with a heavier ram. The velocity of impact of the ram was found to be of major significance in determining the magnitude of the driving stresses.

Finally, it was seen that although there was a close interaction between the pile-soil-cushion system and hammer that no absolute conclusion can be made regarding the suitability of a certain hammer for all piles. Each situation should be considered individually on the basis of a similar approach to the one followed in this study.

Pile Hammer Selection by Driving Stress Analysis

by

Franklin Barrero-Quiroga

A THESIS

submitted to

Oregon State University

in partial fulfillment of
the requirements for the
degree of

Master of Science

June 1974

APPROVED:

Redacted for privacy

Professor of Civil Engineering
in charge of major

Redacted for privacy

Associate Professor of Civil Engineering

Redacted for privacy

Head of Department of Civil Engineering

Redacted for privacy

Dean of Graduate School

Date thesis is presented April 1, 1974

Typed by Mary Jo Stratton for Franklin Barrero-Quiroga

ACKNOWLEDGMENTS

Many persons and institutions contributed directly and indirectly to the evolution and structure of this thesis.

In particular I wish to thank my major professor, Thomas J. McClellan, for his guidance during the preparation of this thesis. I am indebted to my minor professor, Dr. Warren L. Schroeder, who encouraged me with his keen interest in the subject as well as through the arrangements of financial support that made this study possible.

Thanks to Mr. Walter J. Hart, Bridge Engineer of the Oregon State Highway Division, and to Mr. Wilbur F. Peleaux, of the Port of San Francisco, for the valuable information provided for this study.

I wish to gratefully acknowledge the financial support of the Computer Center, the Civil Engineering Department and the Engineering Experiment Station that contributed to the completion of this paper.

TABLE OF CONTENTS

	Page
I. INTRODUCTION	1
II. PURPOSE AND SCOPE	3
III. LITERATURE REVIEW	4
IV. MATHEMATICAL MODEL	8
Wave Propagation Concepts	8
Theory Review	12
Idealization Equations	14
V. ANALYTICAL STUDIES	25
Study Outline	25
Hypothetical Cases	25
Port of San Francisco Case History	27
Oregon State Highway Division Test Pile	32
VI. RESULTS AND DISCUSSION	36
Hypothetical Cases	36
Port of San Francisco Case History	52
Oregon State Highway Division Test Pile	60
VII. SUMMARY AND CONCLUSIONS	70
BIBLIOGRAPHY	73
APPENDIX	77

LIST OF TABLES

Table		Page
1	Summary of results for hypothetical cases.	38
2	Summary of results for hypothetical cases.	39
3	Maximum driving stresses in psi, along a 12" x 12" x 55' prestressed concrete pile, hypothetical case.	44
4	Maximum driving stresses in psi, along a 12" x 12" x 55' prestressed concrete pile, hypothetical case.	45
5	Maximum driving stresses in psi, along a 12" x 12" x 110' prestressed concrete pile, hypothetical case.	48
6	Maximum driving stresses in psi, along a 12" x 12" x 110' prestressed concrete pile, hypothetical case.	49
7	Maximum driving stresses in psi, along a 12" x 12" x 110' prestressed concrete pile, hypothetical case.	50
8	Maximum driving stresses in psi, along a 12" x 12" x 110' prestressed concrete pile, hypothetical case.	51
9	Maximum driving stresses in psi, along a 18" octagonal, 89' prestressed concrete pile, Port of San Francisco Case History.	54
10	Maximum driving stresses in psi, along a 18" octagonal, 89' prestressed concrete pile, Port of San Francisco Case History.	55
11	Maximum driving stresses in psi, along a 18" octagonal, 89' prestressed concrete pile, Port of San Francisco Case History.	58

Table		Page
12	Maximum driving stresses in psi, along a 18" octagonal, 80' prestressed concrete pile, Port of San Francisco Case History.	59
13	Maximum driving stresses in psi, along a 12" x 12" x 46' prestressed concrete pile, Oregon State Highway Division Test Pile.	64
14	Maximum driving stresses in psi, along a 12" x 12" x 46' prestressed concrete pile, Oregon State Highway Division Test Pile.	67
15	Maximum driving stresses in psi, along a 12" x 12" x 46' prestressed concrete pile, Oregon State Highway Division Test Pile.	68

LIST OF FIGURES

Figure		Page
1	Idealized sequence of stress wave propagation.	9
2	Idealized reflection of stress wave.	11
3	Propagation and reflection of stress wave.	11
4	Free body diagram for dynamic equilibrium.	13
5	Mathematical model for pile driving analysis.	16
6	Idealization for the spring segment of a pile.	22
7	Ultimate soil resistance versus deformation.	22
8	Flowchart of problems for hypothetical cases.	26
9	Flowchart of problems for Port of San Francisco Case History. Variables: hammer, stiffnes K_2 and soil embedment.	28
10	Flowchart of problems for Port of San Francisco Case History. Variables: soil damping.	30
11	Flowchart of problems for Port of San Francisco Case History. Variables: quake.	31
12	Flowchart of problems for Oregon State Highway Division Test Pile. Variables: hammer and depth of embedment.	33
13	Flowchart of problems for Oregon State Highway Division Test Pile. Variables: hammer and soil resistance.	34
14	Maximum tensile stresses for 55-foot pile, hypothetical case. (a) 10 feet of embedment (b) 55 feet of embedment	 41 42

Figure		Page
15	Maximum tensile stresses in an 89-foot prestressed concrete pile. Port of San Francisco Case History.	57
16	Ultimate soil resistances for Oregon State Highway Division Test Pile.	61
17	Driving record for Oregon State Highway Division Test Pile.	62
18	Maximum tensile stresses for Oregon State Highway Division Test Pile.	66

PILE HAMMER SELECTION BY DRIVING STRESS ANALYSIS

I. INTRODUCTION

During the process of driving prestressed concrete piles, failure of the concrete may occur due to one or a combination of the following causes:

1. Excessively high compressive stresses at the head of the pile.
2. Excessively high compressive stresses at the tip of the pile.
3. Excessive shear stresses created by torsion.
4. Excessive tensile stresses that may occur at certain points in the pile.

The first two causes produce spalling of the pile at its head and tip respectively. The third cause produces spiral cracking of the concrete. The last cause produces transverse cracking of the concrete, and it will be the subject of this study.

Numerous cases (2, 21, 23) of transverse cracking on prestressed concrete piles during driving have been reported. The cracking occurred mainly during the early stages of driving. In some instances the cracking of the concrete was avoided by making some changes in the driving technique; for example, reducing the stroke of the hammer, or using a softer cushion or avoiding jetting before driving.

Certainly the conditions under which tensile cracking occurs are intimately related to the driving hammer. The decision to use a certain kind of hammer should be based on economical and technical considerations. It has been suggested that double acting hammers are unsatisfactory for driving prestressed concrete piles and that single acting hammers are less dangerous (22). This contention in certain cases may be true, but there still exists the problem of deciding which kind of hammer will perform better, in terms of efficiency of driving without damaging the pile. For example, a given pile may be driven safely with a given hammer, say a single acting hammer of a given energy, but the rate of driving may not be sufficiently fast, to the point of making the piling process uneconomical. On the other hand, the opposite extreme is to use another kind of hammer that gives a high penetration rate, as a result a quicker driving operation, but at the expense of the integrity of the pile. Therefore, the question that arises is how to determine which kind of hammer is better suited to perform a given job. One of the answers lies with the experience that foundation engineers may have with equipment used with different types of piles and soils. However, this is not a quantitative way to relate the pile-soil system to the driving equipment, nor is it a reliable one. It appears necessary to understand the mechanics of pile driving to predict the behavior of the hammer-pile-soil system.

II. PURPOSE AND SCOPE

The purpose of this study was to compare potentially damaging effects of a double acting steam-air hammer on a prestressed concrete pile to those of a single acting hammer of the same rated energy.

To accomplish this purpose use is made of the wave equation to determine the driving stresses that the hammer induces in the pile. Parameter studies were made on a group of problems with hypothetical data and on a second group of problems from case histories. In the first set of analyses, double acting and single acting steam-air hammers of the same energy were assumed. For each case the influence of pile length, depth of embedment, cushion stiffness, soil resistance and percentage of soil resistance at the tip of the pile was studied. In the second group, representative of actual problems, hammer type and soil conditions for a given hammer were varied.

III. LITERATURE REVIEW

Several authors have suggested the need to recognize that pile driving problems should be analyzed using dynamic methods. Most of the effort put forth has been directed to answering questions related to the load carrying capacity of a pile. Chellis (3) reports 38 pile driving formulas and the editors of the Engineering News Record have on file more than 400 formulas for the same purpose. Many of them work well in particular situations. There are still more formulas that are being proposed from time to time.

The formulas that have been proposed can be classified in three groups:

a) Empirical formulas, based on statistical investigation of pile driving experiences.

b) Static formulas, based on the side friction and point bearing resistance, which in turn depend on the properties of soils.

c) Dynamic formulas which assume that dynamic pile driving resistance is equal to the static load carrying capacity.

None of the pile formulas takes into consideration all of the factors that are involved in the process of driving. For example, the Hiley formula, often called the "complete formula," takes into consideration several important factors such as the weight of hammer ram, weight of pile, energy of hammer, coefficient of restitution,

etc., but neglects others such as the velocity of the ram, and soil damping, to name two. Furthermore, none of the formulas produces a prediction of the driving stresses along the pile.

Isaacs (17) is credited with having been the first to observe that propagation of driving stresses in a pile may be analyzed by the wave equation. Fox (10) proposed an exact solution to be used for pile-driving analysis. Later, Glanville, Grime, Fox and Davies (13) published the first correlations between experimental studies and the results obtained by Fox's proposed solution to the wave equation. Fox's solution was too complex to be used in real cases. It was necessary to make simplifying assumptions, such as zero frictional side resistance and a perfectly elastic cushion block. Nevertheless, from their experimental work and Fox's solution, they concluded that their results were in agreement.

Cummings (5) worked with the wave equation as developed by Fox, but he arrived at the same conclusion; that the expressions were too complicated to be used in real cases and even for simple problems the amount of work involved for the solution was still considerable.

Because a real problem of pile driving analysis involves many variables, such as the side frictional soil resistance, the soil damping parameters and other factors that prevent solving the wave equation directly, it was necessary to obtain expressions, based on wave propagation concepts, in which these parameters could be represented.

Smith (26) proposed a mathematical model and its corresponding numerical analysis which accounted for many of the parameters involved in pile driving. He continued updating his work (27, 28, 29, 30, 31). However, his works received little attention from the profession until 1960 (32) when he published a summary of his works. In this summary he recommended typical values of soil parameters for use in his solutions. This publication represented a breakthrough in the pile-analysis problem and two immediate applications to the wave equation were suggested:

1) A way to estimate the ultimate driving resistance and to predict driving stresses.
2) Parameter studies to determine the influence of the variables that are involved in pile driving.

The second application is useful when a better understanding of the mechanics of a pile driving problem is needed and when some variables in the problem are not well defined. In this case ranges of results can be obtained. Since the Smith paper, extensive research has been carried out at Texas A and M University in joint effort with the Texas Transportation Institute and the Federal Highway Administration, under the direction of C. H. Samson (24). Forehand and Reese (8) worked with the wave equation at Princeton University. They arrived at conclusions similar to those of Samson and associates. Both groups used computer programs based on Smith's work. At

present there is no doubt about the applicability of the Smith model. Samson, Hirsch, Lowery and associates have continued working, supplementing the theoretical with experimental work (14, 15, 16, 20, 25). Researchers at Texas A and M University extended Smith's original solution. They studied the influence of the size of the ram and modified the program to include parameters that were more general; for example the cushion in their solution could have nonlinear stress-strain behavior. Hirsch and associates modified the expression to account for damping.

Edwards (7) wrote a computer program based on Smith's procedure. This program gives results within 0.1% of Smith's original program.

Soil damping and quake to be used in the analysis have been suggested by Forehand and Reese (9). Bowles (1) also gives a way to evaluate the damping values from laboratory tests. The most recent work in this field has been done by Coyle (4) and associates, who found nearly the same values for damping and quake as those proposed by Smith. More work needs to be done to determine soil parameters than can be used reliably.

IV. MATHEMATICAL MODEL

Wave Propagation Concepts

For purposes of continuity a brief review of the phenomenon of impact in slender bars is given here as applied to prestressed concrete piles. For more detailed aspects the reader is referred to references (6) and (34).

When a slender bar is hit on one end by a weight in a short period of time, the head of the bar will be subject to a compressive stress caused by the impact. This compressive stress travels to the other end of the bar. If the weight hits the bar instantaneously and the impact remains constant for a period of time and assuming that weight and bar are rigid, the stresses build up in the sequence shown in Fig. 1, where Δt is a convenient time interval.

When the weight hits the bar, the increase of stress at the head of the bar is sudden. Fig. 1 (c) shows an instant Δt later. By this time the stresses have traveled down the bar a certain distance, with a speed, c. Fig. 1 (e) corresponds to the instant in which the hammer ceases to press the bar head. The front of the compressive stresses will have traveled a certain distance, $c \times 4\,\Delta t$, during this period. The length of this stressed zone is L_s. This length will depend on the time that the hammer acts on the bar, as well as on the

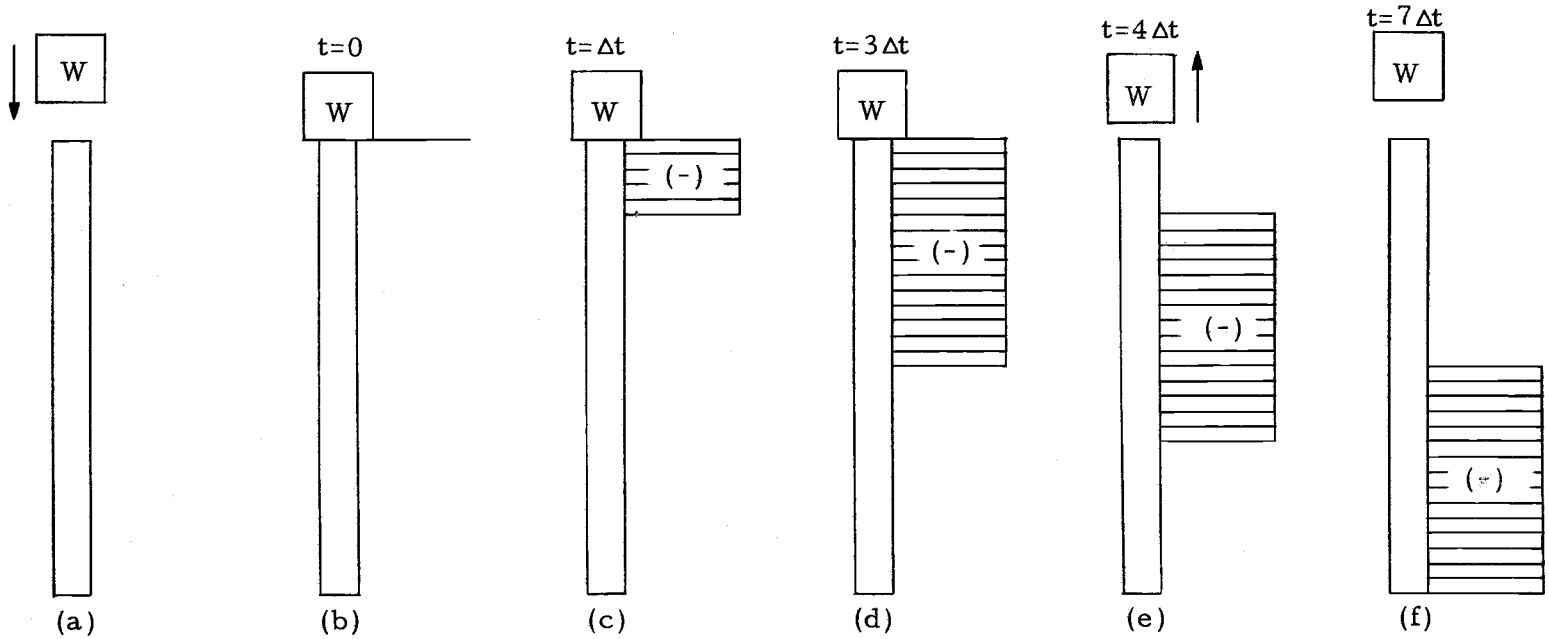

Figure 1. Idealized sequence of stress wave propagation.

speed of propagation of the stress, which in turn depends on the kind of material of the bar. Fig. 1 (f) shows the instant when the front of the stress wave reaches the end of the bar. From this point on, two extreme developments are possible, depending on whether the end of the bar is fixed or free. If this end is free, the stress wave will "reflect" as tensile wave. This phenomenon is illustrated by Smith (31). He compares the pile to billiard balls lined up and tied together in some way. If the first ball is struck with the cue ball it is evident that the impact will transmit to the last ball through the intermediate ones. The last ball will try to shoot off by itself with a velocity approximately equal to the cue ball, but as it is tied to the other ball this one will try to follow the motion of the first one. In turn the next to the last ball will pull the preceding one and so on. The pulling action produces the tensile stresses.

If the end is fixed and assuming the bar has no friction on its sides, at an instant later than 6 Δt of Fig. 1 (f), the wave will reflect as a compression wave and for ideal conditions the total stress at the tip will be double that of the top of the pile. Fig. 2 (a) and (b) illustrate each case.

In a real situation the impact does not happen instantaneously and the build up of stresses is gradual. A more realistic representation of stresses corresponding to Fig. 1 (e) and Fig. 2 (a) and (b) is given in Fig. 3.

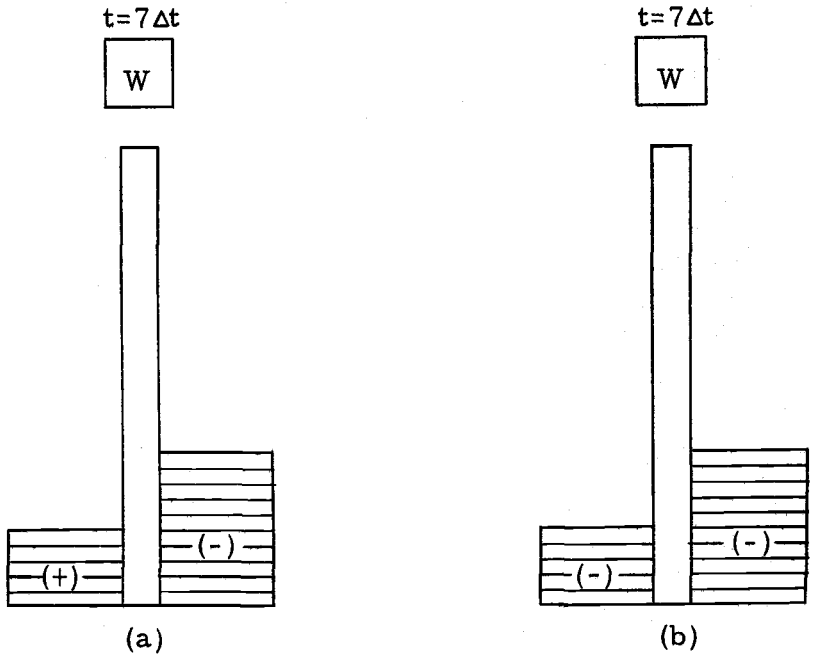

Figure 2. Idealized reflection of stress wave.
(a) Free end, (b) Fixed end.

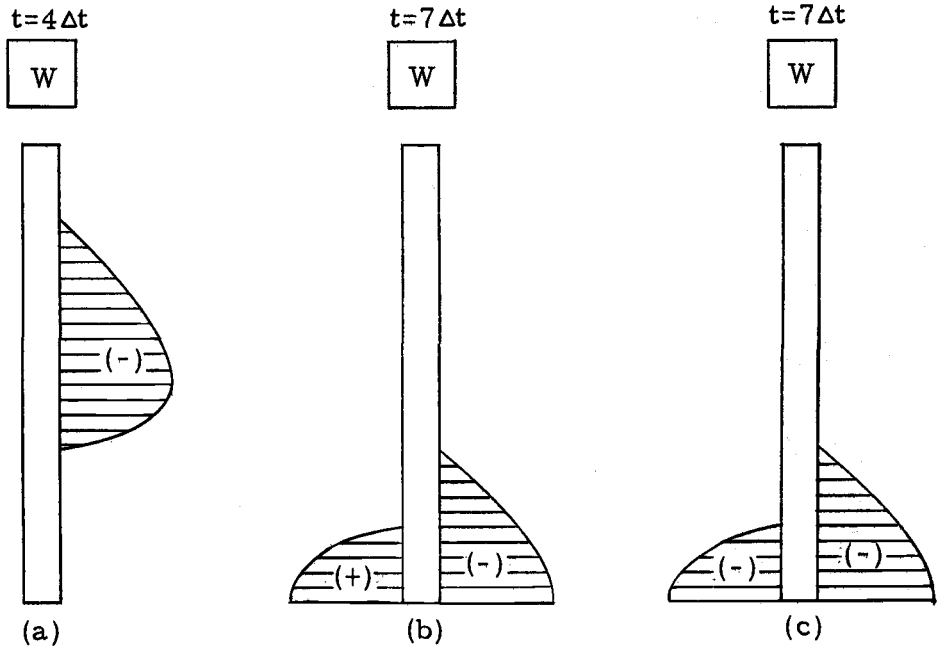

Figure 3. Propagation and reflection of stress wave.

Theory Review

Timoshenko (34) presents a derivation of the wave equation from the dynamic equilibrium of the shaded portion in Fig. 4. The stressed element shown in Fig. 4 (a) travels along the bar at velocity c, producing axial displacements, u. Stresses on the element are shown in Fig. 4 (b). Horizontal summation of forces gives

$$-\sigma_x A + \sigma_x A + \frac{\partial \sigma_x}{\partial x} dxA - ma = 0 \qquad (1)$$

where

$$m = Adx\rho$$

and ρ is the mass per unit volume of the bar.

The acceleration of the mass is

$$a = \frac{\partial^2 u}{\partial t^2}$$

Substituting m and a in Eq. (1) and simplifying:

$$\frac{\partial \sigma_x}{\partial x} = \rho \frac{\partial^2 u}{\partial t^2} \qquad (2)$$

But, by definition

$$\epsilon_x = \frac{\partial u}{\partial x}$$

$$\sigma_x = E\epsilon_x$$

Substituting ϵ_x and σ_x in Eq. (2):

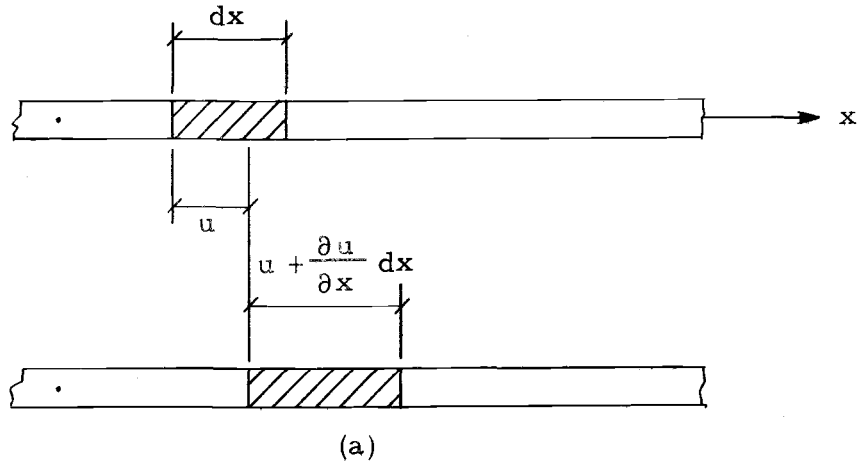

(a)

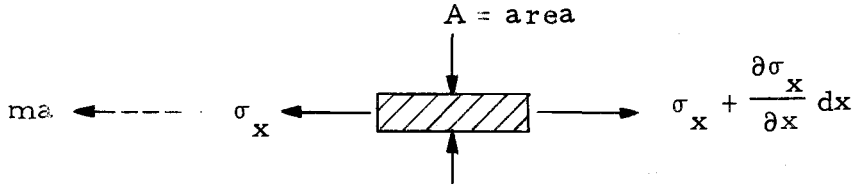

(b)

Figure 4. Free body diagram for dynamic equilibrium.

$$\frac{\partial^2 u}{\partial t^2} = \frac{E}{\rho} \frac{\partial^2 u}{\partial x^2} \tag{3}$$

Eq. (3) is the one dimensional wave equation for stress propagation in a bar with no friction on the sides.

For friction acting on the sides of the element

$$\frac{\partial^2 u}{\partial t^2} = c^2 \frac{\partial^2 u}{\partial x^2} \pm R \tag{4}$$

where c is the velocity of wave propagation and R is soil resistance per unit mass of pile.

Idealization Equations

Because the solution to Eq. 4 was very cumbersome without the aid of electronic computers (10), its application was limited to ideal cases or to a few real problems for which very drastic simplifying assumptions were necessary to make.

Smith proposed a model to represent the hammer-pile-soil system (32). This idealization consists of a simulation of the soil medium, the hammer and the pile and the cushion blocks (7). The hammer and pile are idealized by a system of discrete weights connected with massless springs. The springs represent the stiffnesses of the pile, and sometimes the ram and the cushion blocks. Because the cushion blocks have very small weights, these are neglected and only its spring action is considered. The soil resistance is simulated

by a spring and a damper acting on each pile segment.

In Fig. 5, $W_{(1)}$ is the weight of the ram, $W_{(2)}$ is the weight of the pile cap, and $W_{(3)}$ through $W_{(8)}$ are the weights of each segment of pile. $K_{(1)}$ is the spring representing the stiffness of the cushion between the ram and pile cap. $K_{(2)}$ represents the combined stiffness of the cushion between the pile cap and first segment of pile and the stiffness of this first segment. $K_{(3)}$ through $K_{(7)}$ are the stiffnesses of the pile segments. $K'_{(5)}$ through $K'_{(8)}$ are the stiffnesses of the side soil springs, while $J'_{(5)}$ through $J'_{(8)}$ are the damping constants of the side soil spring.

In general $W_{(m)}$ represents the weight of mass m, $K_{(m-1)}$ its spring stiffness, $K'_{(m)}$ and $J'_{(m)}$ are the side soil spring and the side damping constant acting on mass m.

Smith proposed a numerical solution for his model (32). This solution was based on a repetitive use of the following equations of motion and equilibrium that he derived for mass m:

$$D_{(m,\,t)} = D_{(m,\,t-1)} + 12\ \Delta t\ V_{(m,\,t-1)} \tag{5}$$

$$C_{(m,\,t)} = D_{(m,\,t)} - D_{(m+1,\,t)} \tag{6}$$

$$F_{(m,\,t)} = C_{(m,\,t)}\ K_{(m)} \tag{7}$$

$$R_{(m,\,t)} = \left[D_{(m,\,t)} - D'_{(m,\,t)}\right] K'_{(m)} \left[1+J_{(m)}\ V_{(m,\,t-1)}\right] \tag{8}$$

$$V_{(m,\,t)} = V_{(m,\,t-1)} + \left[F_{(m-1,\,t)} - F_{(m,\,t)} - R_{(m,\,t)}\right]\frac{g\,\Delta t}{W_{(m)}} \tag{9}$$

where:

m = mass number

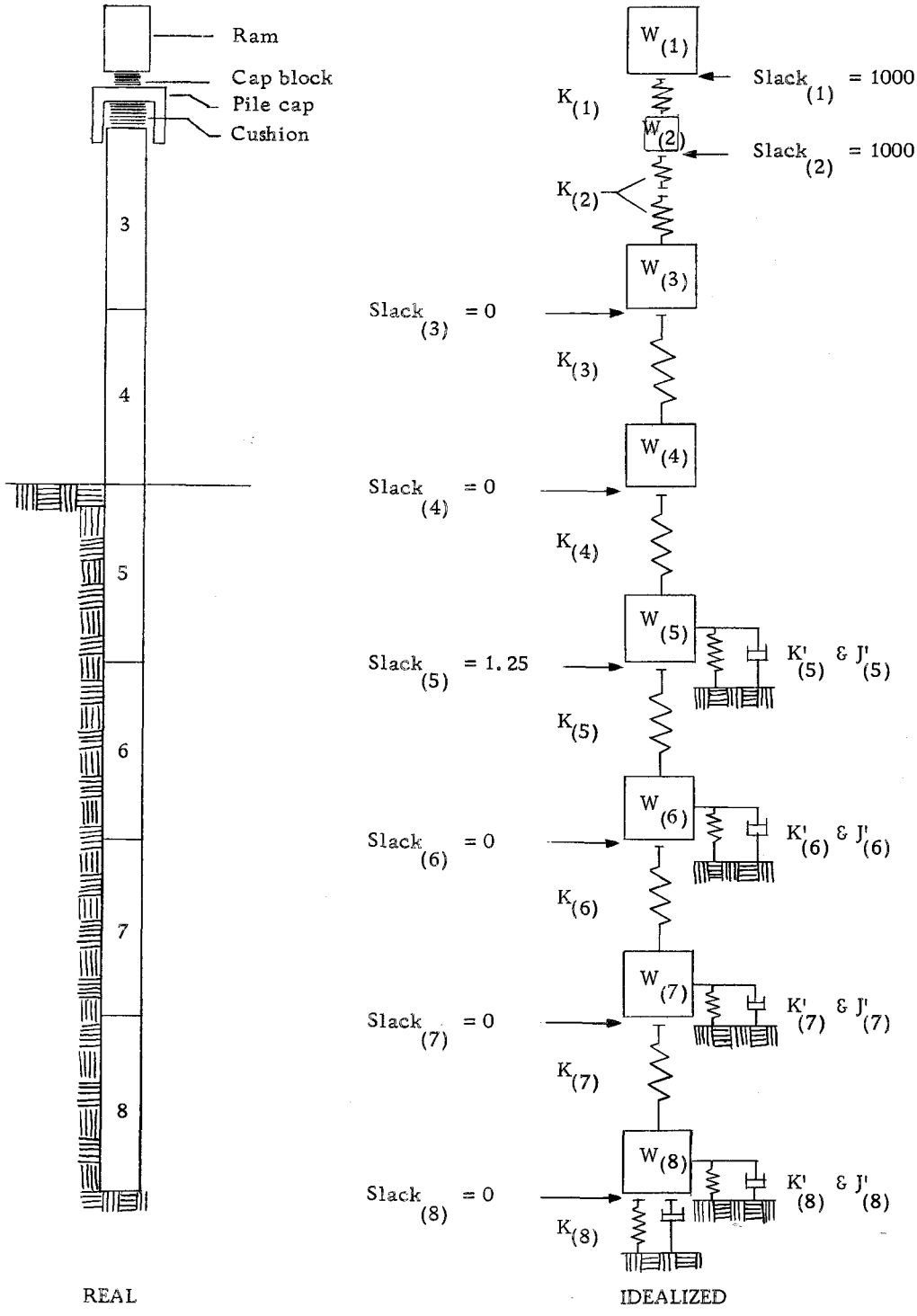

Figure 5. Mathematical model for pile driving analysis.

t = time interval number in which a given value is considered

Δt = size of the time interval (sec)

$D_{(m, t)}$ = total displacement of mass number m during time interval t (in)

$V_{(m, t)}$ = velocity of mass m during time interval t (ft/sec)

$C_{(m, t)}$ = compression of the spring m during time interval t (in)

$F_{(m, t)}$ = force exerted by spring number m between segment numbers (m) and (m+1) during time interval t (lb)

$R_{(m, t)}$ = total soil resistance acting on segment m (lb/in)

$K_{(m)}$ = spring rate of mass m (lb/in)

$K'_{(m)}$ = spring rate of the soil spring causing the external soil resistance force on mass m (lb/in)

$D'_{(m, t)}$ = total inelastic soil displacement or yielding during the time t at segment m (in)

$J_{(m)}$ = damping constant for the soil acting on segment number m (sec/ft)

g = gravitational acceleration (ft/sec^2)

$W_{(m)}$ = weight of segment number m (lb)

It can be shown that by combining Eq. (5), (6), (7), (8), and (9) the following expression can be obtained:

$$D_{(m, t)} = 2D_{(m, t-1)} - D_{(m, t-2)} - \frac{12g\Delta t^2}{W_{(m)}} \left\{ \left[D_{(m-1, t-1)} - D_{(mt-1)} \right] K_{(m-1)} - \left[D_{(m, t-1)} - D_{(m+1, t-1)} \right] \right\} \quad (12)$$

This is a difference form of the wave equation, Eq. (4). Eqs. (5) through (9) are therefore equivalent to the wave equation in its difference form. This is why Smith's method is called the "wave equation method."

In the model shown in Fig. 5, the hammer, pile and soil were directly represented by the weight-spring-dash-pot system. However, in order to be aware of some limitations and simplifications introduced for this particular model, a brief consideration of each of the parts that form the pile-soil-hammer system is given below.

Hammer. Basically there are five kinds of hammers: drop hammer, single acting hammer, double acting hammer, differential hammer, and vibratory hammer (11). This writer is aware that only the first four kinds of hammers have been simulated in the numerical solution of the wave equation for pile driving analysis (7, 8, 20). This study was limited to single acting and double acting steam-air hammers.

In the single acting hammer the energy delivered to the pile comes entirely from the weight of the ram. Compressed air or steam lifts the ram to a certain height, after which the ram drops with an energy equal to the potential energy that the ram acquired when it was lifted, minus any energy losses.

In the double acting steam-air hammers the energy to drive the pile comes from the potential energy of the ram plus the energy of the

steam-air that pushes the ram from the top of its stroke. Again, energy losses take place.

The differential acting steam-air hammer works basically in the same way as double acting hammers, but there is a cycle arrangement that permits getting a mixture of characteristics of the single acting hammers and double acting hammers. There are advantages and disadvantages for each kind of hammer.

As far as the idealization of the hammers to be simulated in the wave equation, there is no difference. The ram can be divided into a number of segments with spring constants, as the pile is divided, but investigation made by Hirsch, Lowery and Samson (20) showed that there was very little difference in the driving stresses and maximum point displacement when the ram was divided into ten segments as compared to those stresses and displacements when the ram was considered as a whole. Based on these findings, the ram weight in this study will be considered concentrated in one segment having an infinite stiffness relative to the stiffnesses of the rest of the system.

Although the manufacturers of pile driving equipment furnish maximum energy rating for their hammers, the actual available energy is less. There are several reasons for this. Among them are poor hammer conditions, lack of lubrication and wear. Chellis (3) and Edwards (7) give some recommended values of efficiency for different hammers. For this study an efficiency of 100% was assumed for the hammers.

Cushions. The cushions are needed to limit the driving stresses in hammer and pile. There are two characteristics pertaining to the cushions that are important in the pile driving analysis by the wave equation. They are stiffness and coefficient of restitution. The stiffness is rather simple to control, at least initially. The modulus of elasticity of the cushion, its area and thickness control the stiffness. Smith (32) proposed a linear variation for the strain-stress relationship. Hirsch and associates (20) found that the variation should be a curve. They proposed a parabolic curve for the loading portion and a linear variation for the unloading. They also concluded that the dynamic stress-strain relation is very similar to the static one. From the stress-strain relations found with the wave equation, they determined coefficients of restitution for several materials. However, since the thickness of wood cushions, for example, change considerably as it is used, it seems very difficult to predict the real stress-strain relationship corresponding to each thickness. Based on the above considerations, the assumption of linear stress-strain relations for cushions seems to be reasonable, for the purposes of this study.

Pile. The length of segments in which the pile is divided is usually 5 feet to 10 feet. The length of each segment is related to the time interval used for each cycle of calculations, in addition to the material of the pile. For prestressed concrete piles Smith

recommends time intervals of 1/3000 sec for segments of pile between 8 feet and 10 feet long. For smaller segments, the time interval should be reduced proportionally. For the hypothetical part of this study, five foot segments were considered, while for the case histories other convenient segment lengths were taken.

Smith suggested that internal damping in the pile might be significant. He proposed the following expression:

$$F_{(m,\,t)} = C_{(m,\,t)}\,K_{(m)} + \frac{B\,K_{(m)}}{12\,\Delta t}\left[C_{(m,\,t)} - C_{(m,\,t-1)}\right] \qquad (13)$$

where B = 0.002 sec/ft is the internal damping constant (21). The above equation was derived from the model shown in Fig. 6 (b). Hirsch, using the concept of static modulus of elasticity, E, and sonic modulus of elasticity introduced the model of Fig. 6(c), for which he derived the expressions for including the effects of damping.

The maximum stresses found in the pile usually occur during the first or second pass of the stress wave along the pile. During this time the effects of damping are small and they can be neglected (20). Experimental results confirm this theoretical conclusion. For this reason model of Fig. 6 (a) will be assumed for the present study. However, for timber piles, this may not be true since its damping capacity is much higher than for steel and concrete (20).

Soil Parameters. Possibly dynamic soil resistance is the least known of all factors involved in pile driving analysis. Smith (32)

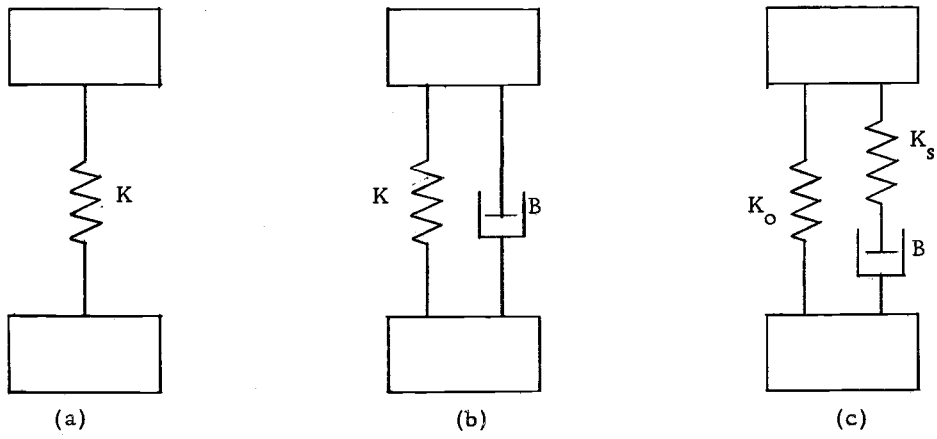

Figure 6. Idealizations for the spring segment of a pile. (a) no damping present, (b) and (c) damping is present.

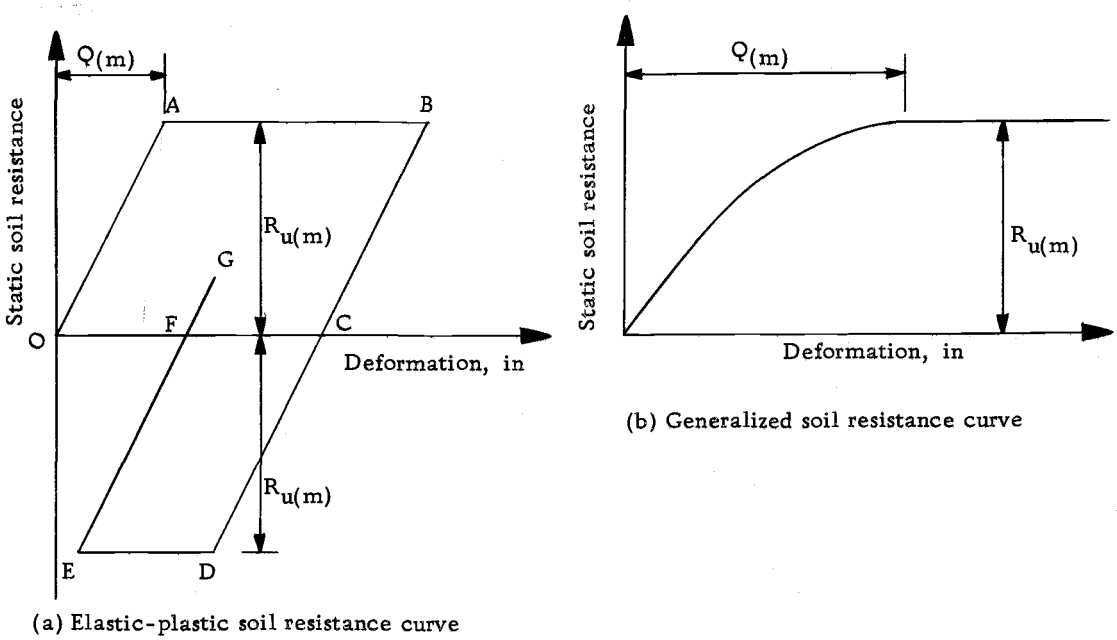

(a) Elastic-plastic soil resistance curve

(b) Generalized soil resistance curve

Figure 7. Ultimate soil resistance versus deformation.

proposed Fig. 7 (a) to define the soil deformation-static resistance.

Fig. 7 does not include the dynamic soil properties necessary for pile driving analysis. The resistance function shown is only defined by $Q_{(m)}$ (ground quake or rebound) and the ultimate static soil resistance $R_{u(m)}$ of the pile. Path OABCDEFG represents the load deformation characteristics of the soil along the pile when the pile moves downward, or upward. However, for the soil located at the tip of the pile, only path OABCFG is appropriate, since no forces downward will be present at the tip as the pile rebounds. The spring constant for the curve between O and A can be defined as:

$$K'_{(m)} = \frac{R_{u(m)}}{Q_{(m)}}$$

To include the damping effects of the soil, a third value, $J_{(m)}$ will be introduced and it is defined as the damping constant of the soil spring (m). The total resistance of the soil including the effect of loading rate is given by:

$$R_{(m,\,t)} = [D_{(m,\,t)} - D'_{(m,\,t)}]K'_{(m)}[1 + J_{(m)}\ V_{(m,\,t-1)}]$$

which was one of the group of equations developed by Smith.

Hirsch (20) worked with a nonlinear relationship for the soil. Fig. 7 (b) shows such variation of deformations and static load resistances. He found there was very little difference between this approach and the results of assuming an elastic-plastic variation.

Only a drastic change in the soil resistance curve was found to cause an appreciable difference in the solution. For this reason a linear soil resistance curve was used in this study.

V. ANALYTICAL STUDIES

Study outline

The numerical solution of the wave equation permits variation of one or more parameters in the analysis while keeping the others constant. This technique was used for studying the group of problems described in this section.

A group of hypothetical problems was first considered to demonstrate the versatility of the analytical method and to indicate the importance of the influence of the several controlling variables. The second step was to analyze a problem with tension cracking from case records and to show how the problem and its solution are amenable to analysis by the method proposed. Finally, a case is analyzed to show how the selection of an acceptable hammer from the standpoint of tension cracking might be made.

For all analysis work, the wave equation program developed by T. C. Edwards (9) at Texas A and M University was used.

Hypothetical cases

The variation in the magnitude of the driving stresses under different conditions was considered for the cases described below.

Two types of hammers were assumed: a differential acting steam-air hammer (Super Vulcan 65C) with 19, 200 lb-ft of energy

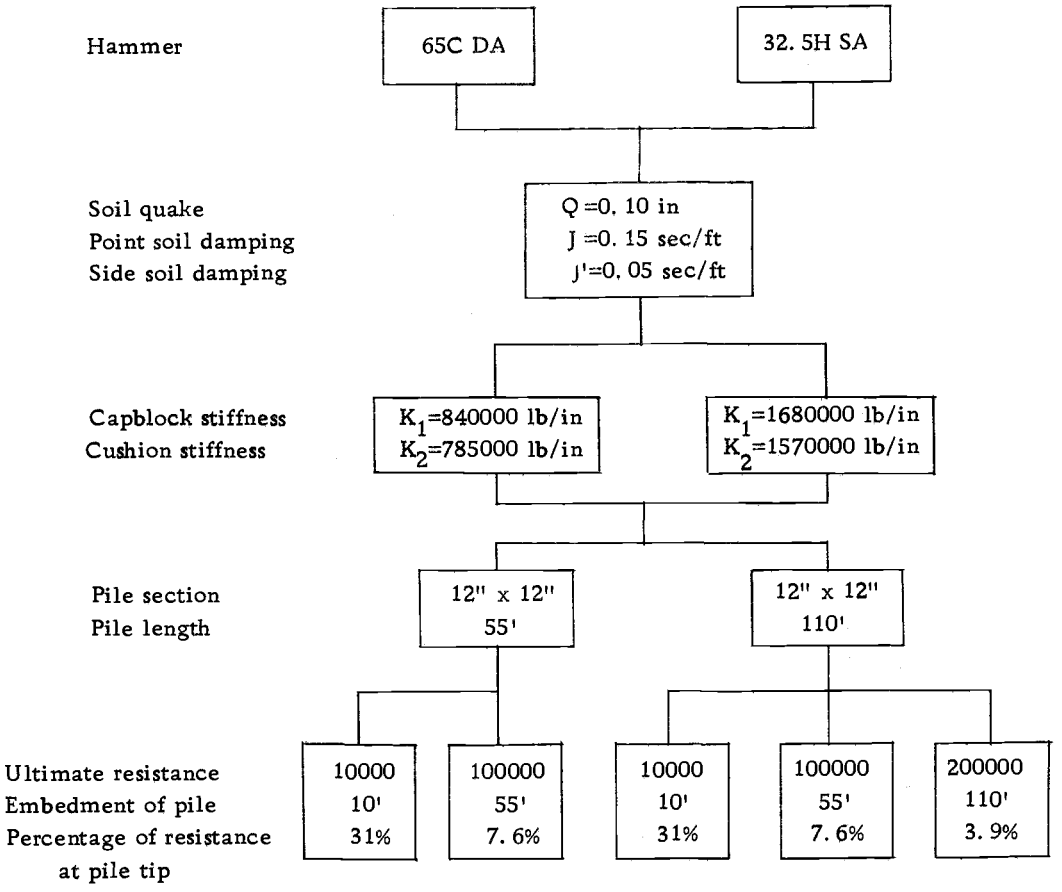

Figure 8. Flowchart of problems for hypothetical cases.

and a ram weight of 6,500 lb, and a hypothetical single acting steam-air hammer with 19, 200 lb-ft of energy and ram weight of 3, 250 lb. The latter will be referred as the 32. 5H SA.

It was assumed that each type of hammer was to drive two 12-inch square prestressed concrete piles; one 55 feet and one 110 feet long.

For each combination of hammer and pile, two different sets of cushions were to be used. One of the sets had a stiffness equal to twice the stiffness of the other.

For the 55-foot long pile, depths of embedment of 10 feet and 55 feet were assumed to represent two extreme situations, while for the 110 foot long pile, the depths of embedment were 10 feet, 55 feet and 110 feet.

For all combinations of situations considered in this group of hypothetical problems, the values of the soil quake and damping factors were considered constant.

Fig. 8 shows the organization for this set of 20 problems.

Port of San Francisco Case History

Prestressed concrete piles 67 feet to 89 feet long were used in the substructure for the dock at Army Street Pier, Port of San Francisco. In the process of driving the 18-inch octagonal piles, tension cracking occurred in piles driven with a double acting

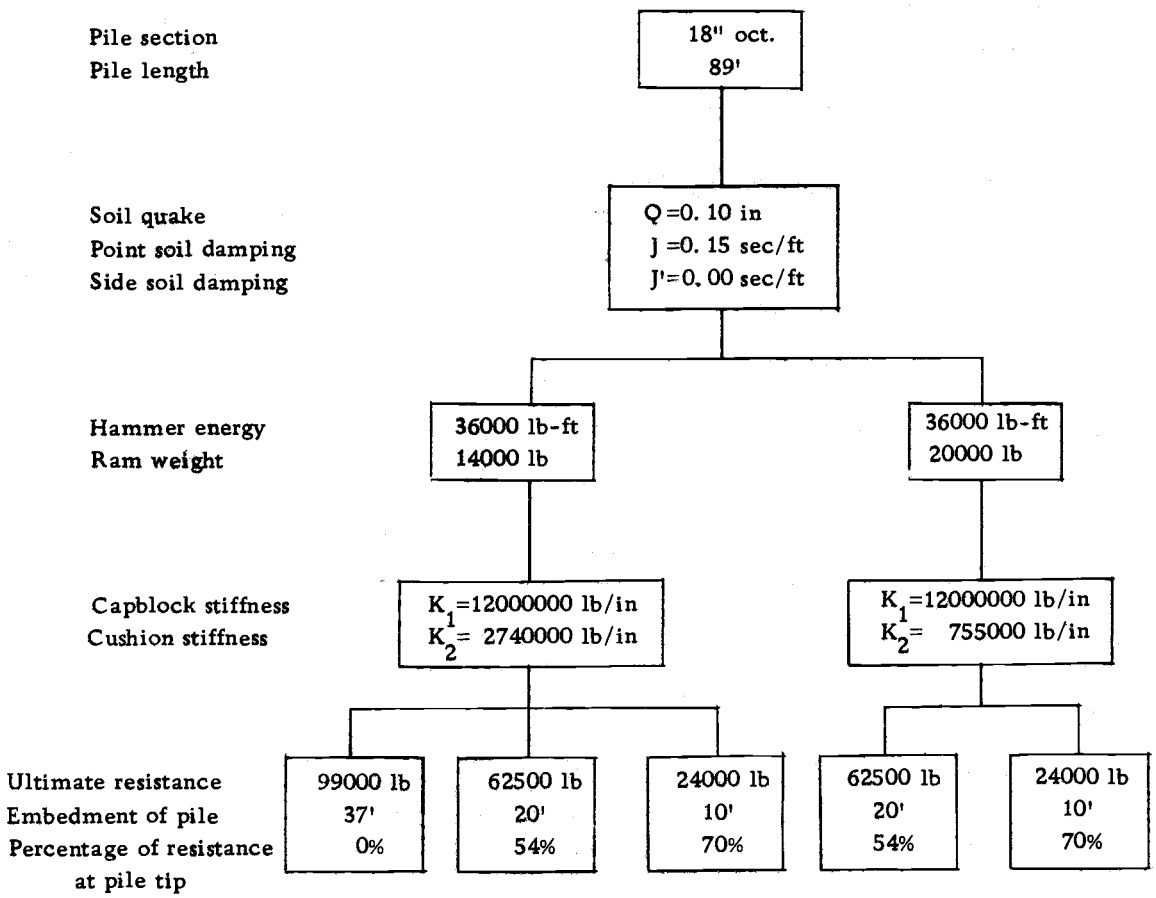

Figure 9. Flowchart of problems for Port of San Francisco Case History. Variables: hammer, stiffness K_2 and soil embedment.

steam-air Vulcan 140C hammer. The damaged piles had been jetted to within 3 feet of final position by jetting through their tips. The cracking problems were avoided by eliminating the jetting, changing the cushion stiffness and increasing the weight of the hammer ram while decreasing its stroke to maintain the same energy as the 140C hammer.

From the records of this job each of the above situations was analyzed and it was determined whether cracking of the piles could have been predicted.

Fig. 9 shows the organization of the problems solved for this case history. The problems are representative of those which occurred in driving piles at the mentioned site.

The 37 feet of embedment corresponds to the depth when driving by the hammer started. Up to this point the piles had been jetted into place. The 10-foot and 20-foot embedments correspond to situations when jetting was not used to drive the pile. The two hammers used had the same energy. However, one had a ram weight of 14, 000 lb and the other had a ram weight of 20,000 lb. For the first case a three-inch thick Douglas-fir plywood cushion was used which was represented by a stiffness of 2, 400, 000 lb/in, while for the second case a 12-inch cushion was used with a correspondent stiffness of 755, 000 lb/in.

Fig. 10 and Fig. 11 show how the soil damping parameters

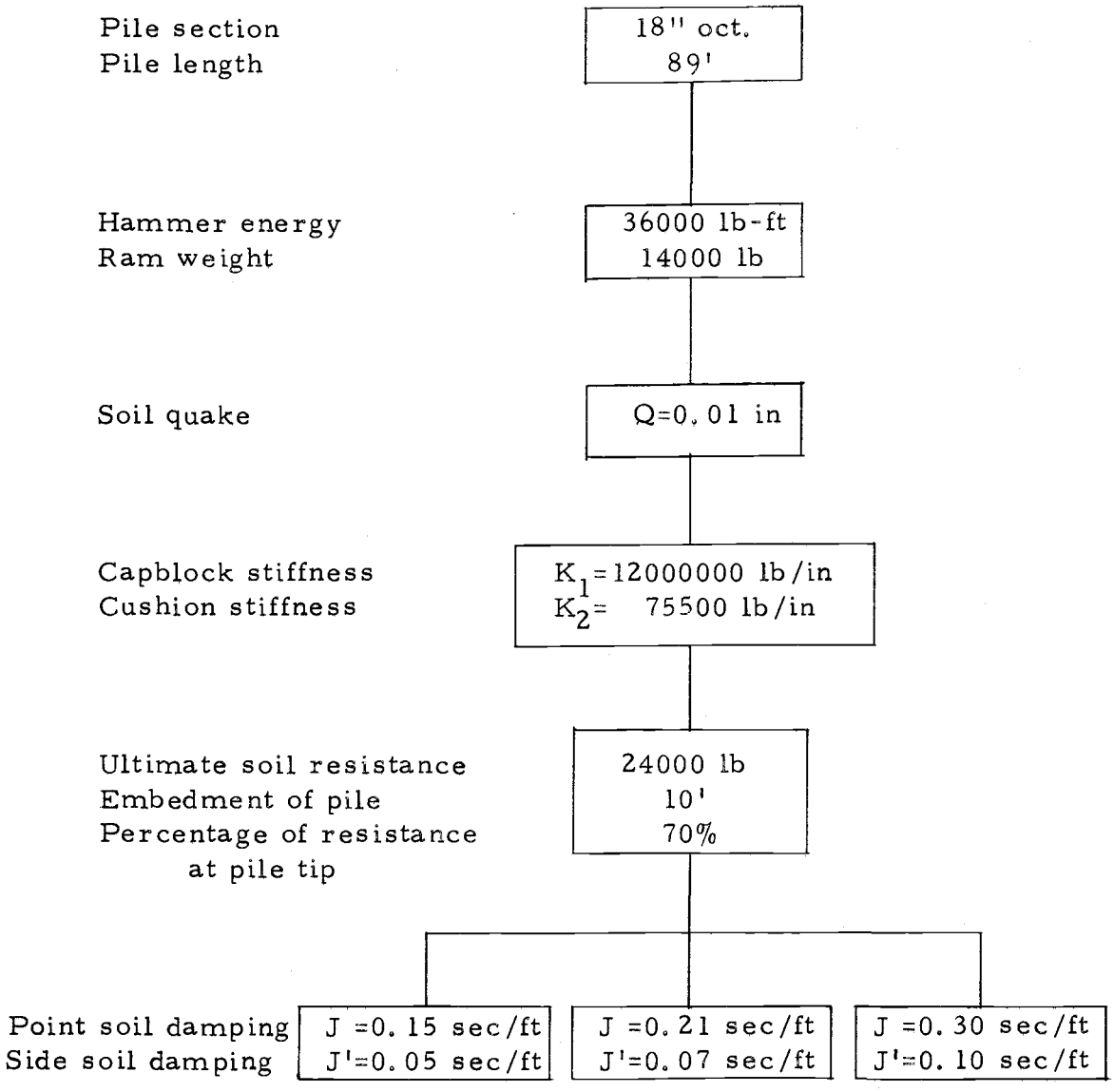

Figure 10. Flowchart of problems for Port of San Francisco Case History. Variable: Soil damping.

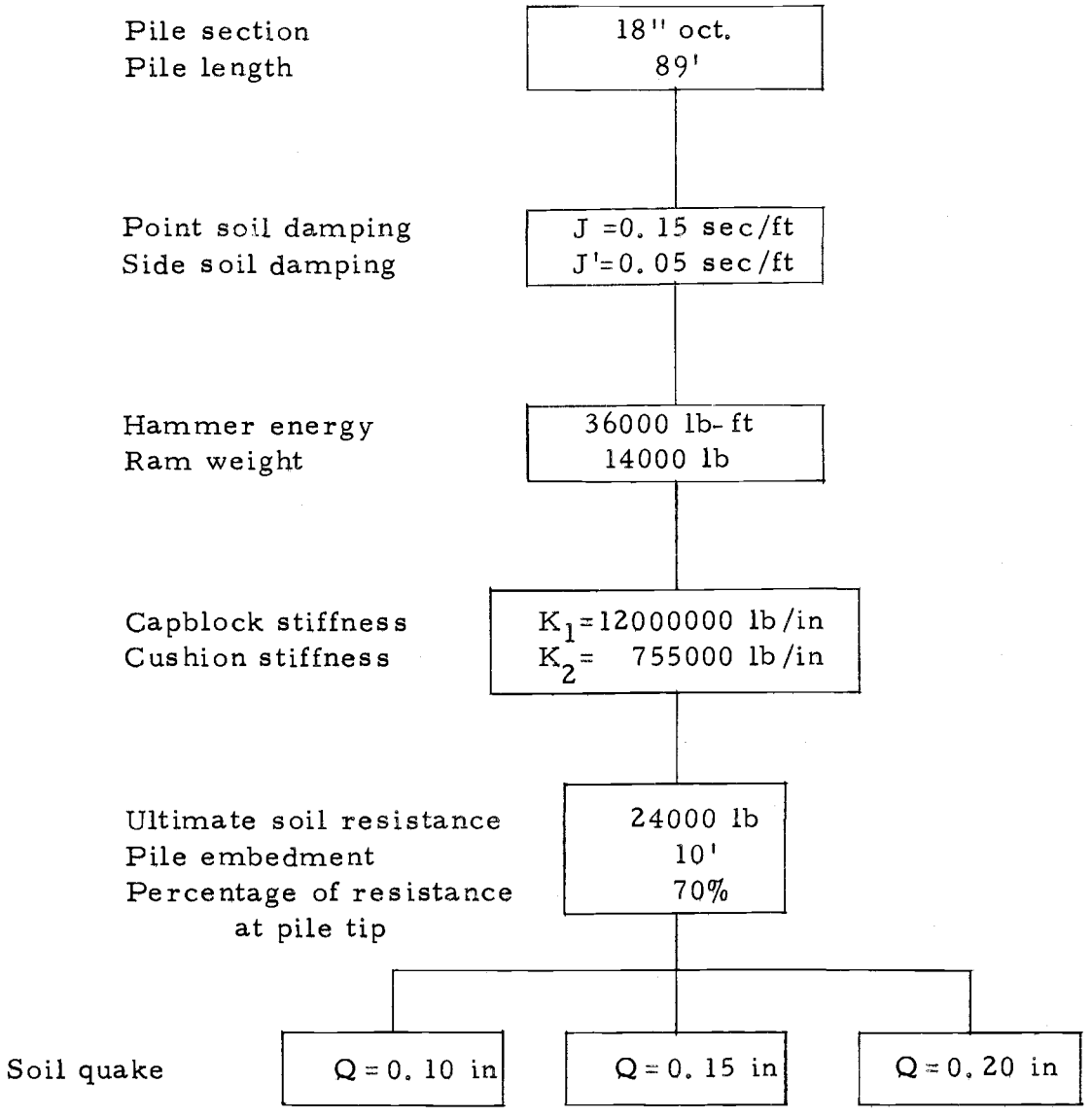

Figure 11. Flowchart of problems for Port of San Francisco Case History. Variable: Quake.

and the quake values were varied to study their influence on the magnitude of the driving stresses.

Oregon State Highway Division Test Pile

The study of potential tension cracking in prestressed concrete piles was made on the basis of the analysis of tensile stresses calculated in a test pile driven for the foundation for the Saint Louis undercrossing bridge on Interstate 5, North of Salem. The pile was 12-inch square, 46-foot long prestressed concrete pile which was driven with a differential acting steam-air Vulcan 65C hammer.

The equipment used to drive this test pile was proposed for use in driving several hundred prestressed concrete piles for other bridge foundations on a recent project. Pile driving specifications did not allow the use of double and differential acting hammers to drive prestressed concrete piles in Oregon. The possibility of tension cracking in the piles is believed to be the basis for this specification.

The present analysis was done to show whether tension cracking should occur for the circumstances under which the test pile was driven, and also under other hypothetical circumstances using a single acting hammer of the same energy but lower ram weight. Fig. 12 sets up the organization of problems solved to determine the

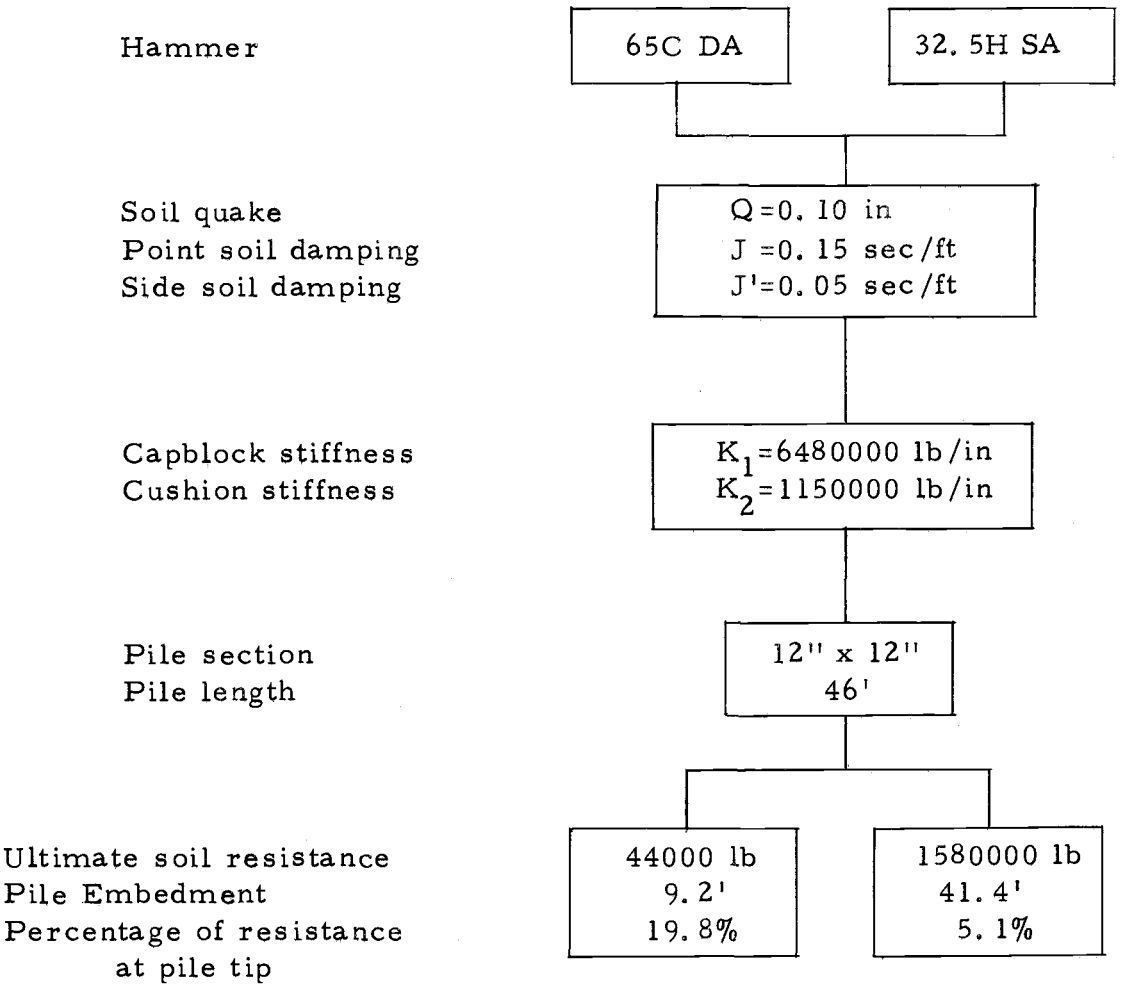

Figure 12. Flowchart of problems for Oregon State Highway Division Test Pile. Variables: Hammer and depth of embedment.

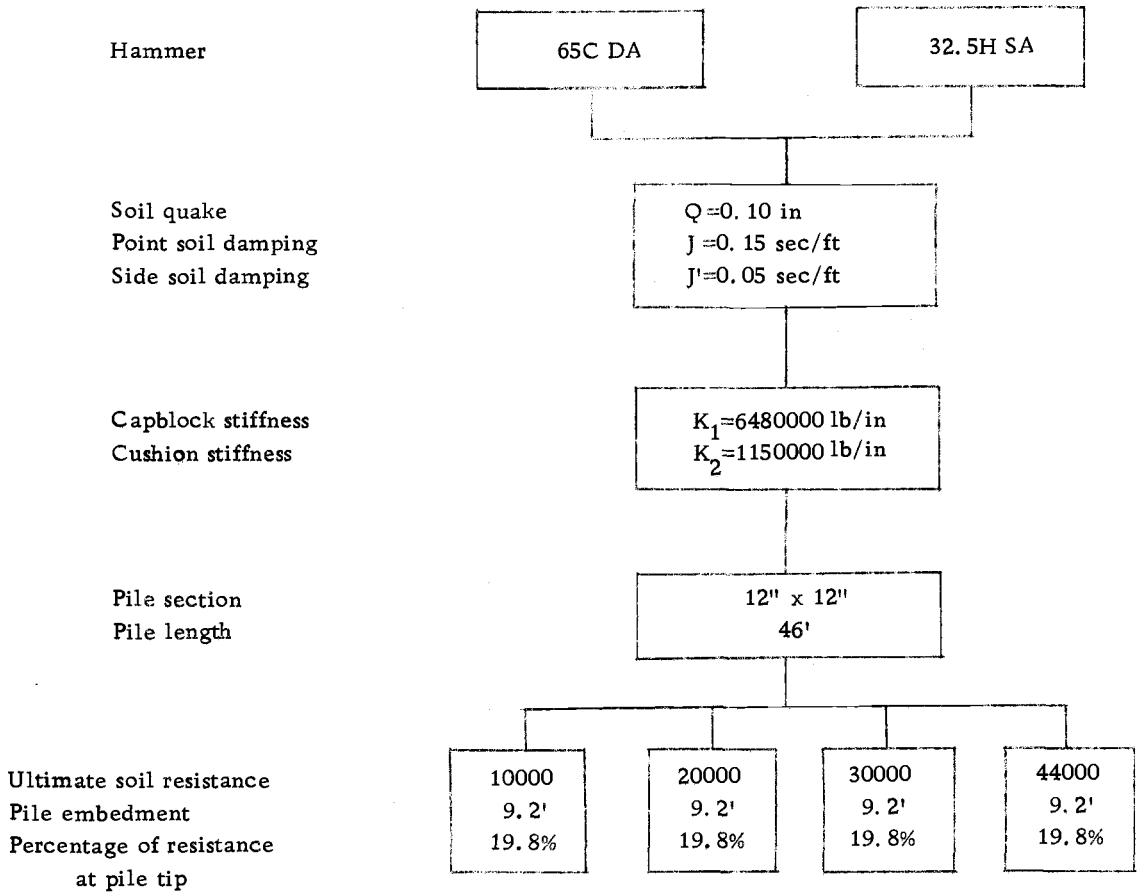

Figure 13. Flowchart of problems for Oregon State Highway Division Test Pile. Variables: hammer and soil resistance.

influence on the magnitude of driving stresses. Depths of embedment of 9.2 feet and 41.4 feet were considered. Fig. 13 shows the outline of problems solved for the two hammers when the ultimate soil resistance varies and the pile embedment remains constant at 9.2 feet below ground level.

VI. RESULTS AND DISCUSSION

The following results and discussion presume that the hammer hits the pile perfectly in the center of its cross section, that the head of the pile is squared and that no torsional effects are induced while driving. All results are for one blow of the hammer. The effects of gravity were included for all cases.

Hypothetical cases

The results obtained for the hypothetical situations shown on the flowchart of Fig. 8 are summarized in Tables 1 and 2. Preliminary solutions had shown that for the same ultimate soil resistance, uniform soil skin friction leads to higher maximum driving stresses than a triangular distribution. The former is appropriate for cohesive soils and the latter proper for granular soils. The results in Tables 1 and 2 are for the uniform skin friction assumption. For comparative purposes any assumption of skin distribution would be valid. The point and side soil damping were assumed to be equal to 0.15 sec/ft and 0.05 sec/ft, respectively, while the quake value was assumed to be 0.10 in. Both assumptions were based on Smith's recommendations (13) and on the work of Coyle and associates (24). To account for the influence of the depth of embedment, for the 55-foot long pile 10 and 55 feet of depths of embedment were

assumed while for the 110-foot long pile, 10, 55 and 110 foot embedments were considered. The ultimate soil resistances were assumed to be as shown below.

Depth of embedment, ft	Ultimate soil resistance, lb	Percentage of resistance at point
10	10,000	31.0
55	100,000	7.6
110	200,000	3.9

The percentages of soil resistance concentrated at the tip of the pile were also assumed. It was felt that computed values for the ultimate soil resistance and its percentage at the pile tip were not necessary for this hypothetical group of problems, since the comparisons pursued can be accomplished from assumed values.

As shown in Tables 1 and 2 the maximum value of the tensile and compressive stresses are consistently higher for the hypothetical single acting hammer than for the double acting hammer. The longer the pile is the higher the driving stresses are. The shallower the depth of embedment, the higher the driving stresses. The higher the stiffnesses of the cushions, the higher the driving stresses.

The permanent set of the pile per blow of the hammer, is considerably larger for the double acting hammer than for the

Table 1. Summary of results for hypothetical cases.

$Q = 0.10$ in, $J = 0.15$ sec/ft, $J' = 0.05$ sec/ft

$K_1 = 840000$ lb/in, $K_2 = 785000$ lb/in

$e_1 = 0.40$, $e_2 = 0.40$

Energy of hammer = 19200 lb-ft

Hammer type	65C DA					32.5H SA				
Length of pile, ft	55		110			55		110		
Embedment, ft	10	55	10	55	110	10	55	10	55	110
R_u, tons	5	50	5	50	100	5	50	5	50	100
% of R_u at tip	31	7.6	31	7.6	3.9	31	7.6	31	7.6	3.9
Maximum tensile stresses, psi	884	718	1584	846	853	1756	1373	2202	1615	1605
Maximum compressive stresses, psi	2005	1984	2002	2100	1984	2298	2272	2298	2378	2271
Permanent set of pile, in	3.63	0.74	3.99	0.86	0.33	2.89	0.48	2.89	0.51	0.21

Table 2. Summary of results for hypothetical cases.

$Q = 0.10$ in, $J = 0.15$ sec/ft, $J' = 0.05$ sec/ft

$K_1 = 1680000$ lb/in, $K_2 = 1570000$ lb/in

$e_1 = 0.40$, $e_2 = 0.40$

Energy of hammer = 19200 lb-ft

Hammer type	65C DA					32.5H SA				
Length of pile, ft	55		110			55		110		
Embedment, ft	10	55	10	55	110	10	55	10	55	110
R_u, tons	5	50	5	50	100	5	50	5	50	110
% of R_u at tip	31	7.6	31	7.6	3.9	31	7.6	31	7.6	3.9
Maximum tensile stresses, psi	1404	1020	2234	1444	1197	2486	1945	2642	2014	1958
Maximum compressive stresses, psi	2576	2540	2574	2629	2539	2982	2957	2982	2982	2956
Permanent set of pile, in	3.68	0.89	3.75	1.00	0.43	2.81	0.59	2.77	0.61	0.27

single acting hammer.

Taking into consideration the maximum tensile stresses and the permanent set per blow, Table 1 suggests that in the case of the 55-foot long pile and with K_1=840, 000 lb/in, K_2=785, 000 lb/in, the double acting hammer would drive more efficiently and with less tensile cracking possibilities than the single acting hammer. However, the same hammer would be dangerous to the same pile under the same conditions if the stiffnesses of the cushions are doubled, as it is indicated in Table 2.

The stiffness of the capblock can actually be quite different from the assumed values but in this analysis the results of Tables 1 and 2 still reflect the different performance expected using the two different hammers.

The influence of the damping in the pile has been neglected, since the maximum driving stresses will occur during the first instants after the blow of the hammer occurred. The segment length for subdividing the pile was taken as 5 feet which is within recommended values (7). By selecting this length problems of instability in the solution were avoided.

Fig. 14 shows that the position of the maximum tensile stresses along the pile is not restricted to any particular area. It shows that the tension cracking can be in the lower, upper or middle third

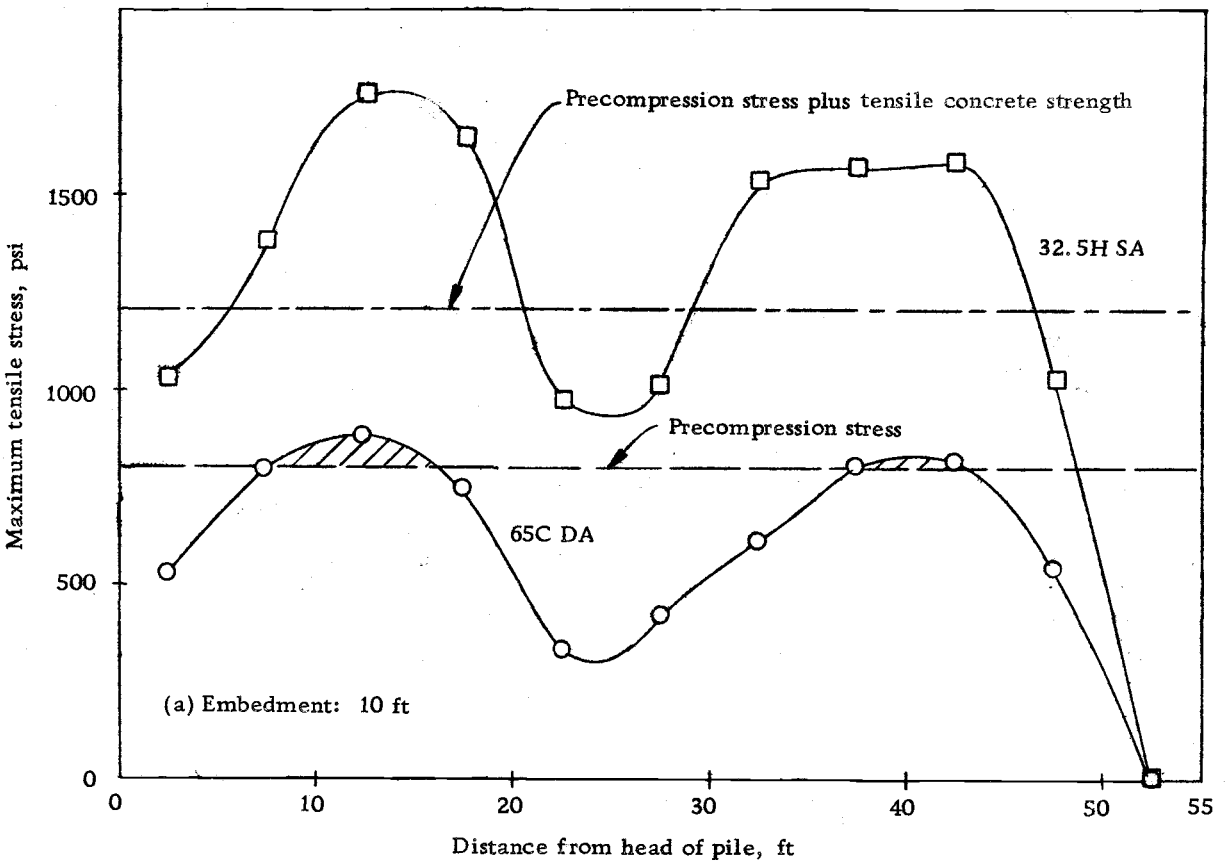

Figure 14. Maximum tensile stresses for 55-foot pile, hypothetical case.

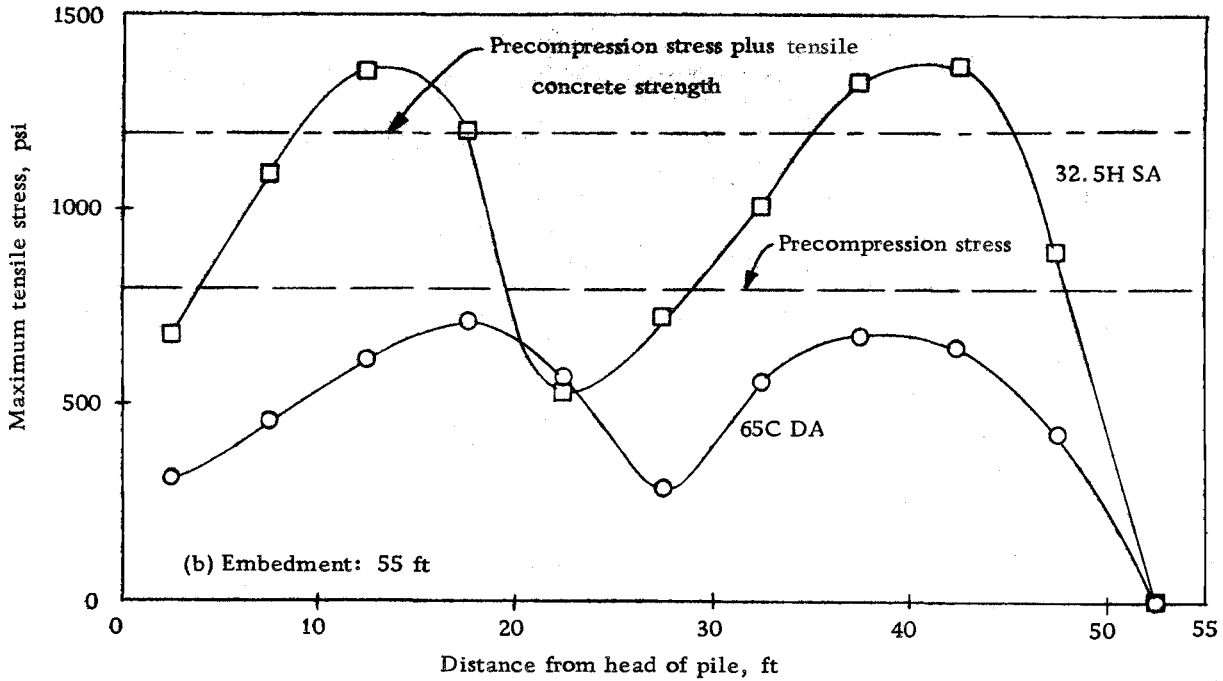

Figure 14. (Continued)

and not only in the upper third of the pile as it has been suggested (12).

For the 65C DA hammer the tensile stresses corresponding to 55 feet of embedment do not exceed the 800 psi precompression from the prestressing operation. Theoretically for this situation the pile will not crack, while it will in the other three situations. It should be pointed out if the pile has not been cracked during handling or by shrinkage, it will be able to withstand tension up to an amount equal to the sum of the precompression stress plus the tensile strength of the concrete. An average value for the ultimate tensile strength of the concrete is $0.08\, f'_c$ (18). For a concrete of 5000 psi and a precompression of 800 psi, the ultimate cracking tensile strength will be 1200 psi. Accounting for the concrete strength, the 65C DA hammer should not cause tensile cracking in the pile. The tensile stresses produced by the 32.5H SA are much higher than the ultimate tensile strength of the concrete plus the precompression stress, and therefore would produce cracking in the concrete.

The position of the cracking zones for the 32.5H SA hammer and 55 feet of pile embedment are shown as shaded areas.

The maximum compressive stresses in the pile for the four situations presented in Fig. 14 are much less than the ultimate

Table 3. Maximum driving stresses in psi, along a 12" x 12" x 55" prestressed concrete pile, hypothetical case.

$Q = 0.10$ in, $J = 0.15$ sec/ft, $J' = 0.05$ sec/ft

$K_1 = 840000$ lb/in, $K_2 = 785000$ lb/in

$e_1 = 0.40$, $e_2 = 0.40$

Type of hammer	65C DA, 19200 lb-ft				32.5H SA, 19200 lb-ft			
Wt. of ram	6500 lb				3250 lb			
Embedment, ft	10		55		10		55	
R_u, lb	10000		100000		10000		100000	
% of R_u at tip	31		7.6		31		7.6	
Distance[a], ft	Tens.	Comp.	Tens.	Comp.	Tens.	Comp.	Tens.	Comp.
5	547	2001	325	1984	1030	2298	584	2272
10	794	2001	465	1947	1380	2297	1096	2231
15	884	2003	622	1910	1756	2297	1361	2190
20	647	2005	718	1872	1633	2298	1200	2150
25	332	2002	577	1824	963	2298	533	2109
30	421	1956	293	1733	1005	2275	731	2044
35	611	1813	566	1567	1533	2171	1003	1900
40	804	1537	681	1310	1566	1891	1330	1629
45	822	1141	651	951	1587	1502	1373	1204
50	547	642	436	525	1023	1072	898	805
55	0	52	0	109	0	56	0	119
Permanent set of pile, in	3.63		0.74		2.89		0.48	

[a]From head of pile.

Table 4. Maximum driving stresses in psi, along a 12" x 12" x 55' prestressed concrete pile, hypothetical case.

$Q = 0.10$ in, $J = 0.15$ sec/ft, $J' = 0.05$ sec/ft

$K_1 = 1680000$ lb/in, $K_2 = 1570000$ lb/in

$e_1 = 0.40$, $e_2 = 0.40$

Type of hammer	65C DA, 19200 lb-ft				32.5H SA, 19200 lb-ft			
Weight of ram	6500 lb				3250 lb			
Embedment, ft	10		55		10		55	
R_u, lb	10000		100000		10000		100000	
% of R_u at tip	31		7.6		31		7.6	
Distance[a], ft	Tens.	Comp.	Tens.	Comp.	Tens.	Comp.	Tens.	Comp.
5	979	2570	628	2540	1310	2982	1074	2957
10	1312	2570	799	2499	1927	2966	1429	2897
15	982	2570	779	2459	1915	2958	1388	2845
20	1404	2572	704	2420	2429	2954	1668	2796
25	1387	2574	801	2383	2486	2951	1945	2752
30	931	2576	566	2345	1982	2949	1481	2710
35	687	2559	397	2289	1091	2935	798	2662
40	1127	2401	657	2120	1883	2840	1362	2531
45	1306	1936	1020	1678	2176	2372	1911	2082
50	1041	1089	715	957	1617	1373	1406	1216
55	0	60	0	130	0	65	0	142
Permanent set of pile, in	3.68		0.89		2.81		0.59	

[a] From head of pile.

compressive strength for the concrete (taken as 0.85 f'_c (19)), which for a 5000 psi concrete is 4250 psi. For this reason they were not shown in Fig. 14.

The results for the rest of the problems for the hypothetical cases are shown in tabular form.

Table 3 shows the maximum values that the stresses take for one blow of hammer. It is seen that if a 55-foot pile is driven with a 65C DA hammer and if the depth of embedment is 10 feet, the maximum compressive stress occurs at 20 feet from the head of the pile. The permanent set of the pile per blow of the hammer is 3.63 in. The same table shows that if the same pile under the same conditions is driven by the hypothetical single acting hammer the maximum compressive stresses increase slightly to 2298 psi, while the maximum tensile stresses increase significantly up to almost double of those of the corresponding double acting hammer case. The permanent set for the second case decreased to 2.89 in/blow, while for the double acting hammer the permanent set was 3.63 in/blow. If the pile was at 55 feet of embedment, the maximum tensile stress and compressive stress would decrease slightly. The permanent set per blow for the 65C DA hammer is 0.74 in, considerably lower than the corresponding permanent set at 10 feet of embedment of the pile. Obviously, the soil resistance is much greater for the deeper embedment.

The only difference in the assumption between the situations in Tables 3 and 4, is the values of the cushion stiffnesses. In Table 4 the stiffnesses of the cushions are double those of the corresponding cases of Table 3. For example, the maximum tensile stress in the pile when the harder cushions were used was 1404 psi and it occurred at 20 feet from the head of the pile, whereas for the softer cushions the maximum tensile stress was 884 psi and it occurred at 15 feet from the head of the pile. The permanent set per blow was slightly affected; the higher values generally corresponded to the stiffer cushions. This observation illustrates the importance of using adequate cushion material and thickness to control driving stresses, but using the minimum required to promote driving efficiency.

Tables 5, 6, 7 and 8 show the maximum tensile and compressive stresses on a 110-foot long pile. Table 5 shows the results corresponding to a differential acting steam-air hammer. Again, the hammer with lower weight of ram and higher velocity of impact causes higher tensile and compressive stresses than a double acting hammer of the same energy. The tensile stresses are particularly sensitive to the differences in impact velocity. The increase in tensile stresses at 10 feet of embedment using a single acting hammer was 39% more than the tensile stresses resulting from using a double acting hammer. At 55 feet of embedment this

Table 5. Maximum driving stresses in psi, along a 12" x 12" x 110' prestressed concrete pile, hypothetical case.

$Q = 0.10$ in, $J = 0.15$ sec/ft, $J' = 0.05$ sec/ft

$K_1 = 840000$ lb/in, $K_2 = 785000$ lb/in

$e_1 = 0.40$, $e_2 = 0.40$

Hammer 65C DA, 19200 lb-ft, Weight of ram = 6500 lb

Embedment, ft	10		55		110	
R_u, lb	10000		100000		200000	
% of R_u at tip	31		7.6		3.9	
Distance[a], ft	Tens.	Comp.	Tens.	Comp.	Tens.	Comp.
5	646	2001	380	2001	287	1984
10	1045	2001	656	2001	460	1945
15	1391	2002	765	2003	500	1906
20	1474	1998	663	2005	398	1867
25	1399	1979	709	2008	488	1829
30	1510	1949	791	2012	591	1790
35	1584	1958	823	2017	685	1752
40	1570	1962	846	2024	679	1714
45	1445	1966	688	2038	589	1676
50	1158	1972	493	2065	571	1639
55	1133	1976	405	2100	499	1602
60	1287	1981	578	2064	627	1565
65	1340	1986	671	2028	740	1530
70	1328	1991	817	1992	853	1496
75	1197	1994	688	1954	678	1461
80	838	1992	384	1903	367	1426
85	833	1943	372	1812	406	1371
90	1018	1806	567	1625	527	1265
95	957	1536	740	1347	739	1073
100	903	1171	728	978	699	785
105	510	692	388	543	396	430
110	0	53	0	112	0	99
Permanent set of pile, in	3.99		0.86		0.33	

[a] From head of pile

Table 6. Maximum driving stresses in psi, along a 12" x 12" x 110' prestressed concrete pile, hypothetical case.

$Q = 0.10$ in, $J = 0.15$ sec/ft, $J' = 0.05$ sec/ft

$K_1 = 840000$ lb/in, $K_2 = 785000$ lb/in

$e_1 = 0.40$, $e_2 = 0.40$

Hammer 32.5H SA, 19200 lb-ft, Weight of ram = 3250 lb

Embedment, ft	10		55		110	
R_u, lb	10000		100000		200000	
% of R_u at tip	31		7.6		3.9	
Distance[a], ft	Tens.	Comp.	Tens.	Comp.	Tens.	Comp.
5	684	2298	521	2298	0	2271
10	1285	2297	868	2297	179	2228
15	1619	2297	974	2297	459	2186
20	1746	2297	1094	2298	730	2145
25	1887	2287	1233	2300	950	2103
30	1988	2254	1319	2302	1092	2063
35	2053	2240	1371	2305	1232	2022
40	2026	2266	1313	2310	1226	1982
45	1783	2278	1038	2320	992	1943
50	1719	2255	895	2342	848	1904
55	1734	2258	996	2378	1112	1865
60	1912	2263	1216	2340	1356	1827
65	2195	2266	1495	2300	1605	1793
70	2202	2269	1615	2261	1600	1759
75	1785	2274	1277	2221	1230	1725
80	978	2274	543	2177	527	1690
85	1061	2253	622	2107	785	1640
90	1511	2147	1017	1957	1188	1542
95	1662	1873	1374	1662	1379	1339
100	1549	1413	1344	1224	1272	998
105	957	792	838	677	788	551
110	0	56	0	121	0	108
Permanent set of pile, in	2.89		0.51		0.21	

[a]From head of pile

Table 7. Maximum driving stresses in psi, along a 12" x 12" x 110' prestressed concrete pile, hypothetical case.

$Q = 0.10$ in, $J = 0.15$ sec/ft, $J' = 0.05$ sec/ft

$K_1 = 1680000$ lb/in, $K_2 = 1570000$ lb/in

$e_1 = 0.40$, $e_2 = 0.40$

Hammer 65C DA, 19200 lb-ft, Weight of ram = 6500 lb

Embedment, ft	10		55		110	
R_u, lb	10000		100000		200000	
% of R_u at tip	31		7.6		3.9	
Distance[a], ft	Tens.	Comp.	Tens.	Comp.	Tens.	Comp.
5	945	2570	746	2570	626	2539
10	1702	2570	1293	2570	1079	2497
15	2154	2570	1444	2570	1197	2455
20	2234	2572	1406	2572	1191	2415
25	2205	2574	1328	2574	1177	2376
30	2207	2572	1286	2576	1169	2338
35	2102	2550	1178	2579	1100	2300
40	2098	2518	1172	2582	1124	2263
45	1941	2525	1062	2586	1101	2227
50	1896	2528	1012	2599	1085	2190
55	1874	2530	880	2629	1059	2154
60	1781	2533	986	2586	1017	2119
65	1680	2536	880	2543	926	2085
70	1506	2538	837	2500	819	2050
75	1452	2542	762	2458	846	2017
80	1518	2545	991	2417	814	1984
85	1160	2546	716	2374	614	1950
90	798	2521	485	2306	402	1904
95	1067	2347	755	2109	854	1761
100	1193	1899	977	1676	952	1424
105	831	1076	678	964	583	823
110	0	60	0	130	0	119
Permanent set of pile, in	3.75		1.01		0.43	

[a]From head of pile

Table 8. Maximum driving stresses in psi, along a 12" x 12" x 110' prestressed concrete pile, hypothetical case.

$Q = 0.10$ in, $J = 0.15$ sec/ft, $J' = 0.05$ sec/ft

$K_1 = 1680000$ lb/in, $K_2 = 1570000$ lb/in

$e_1 = 0.40$, $e_2 = 0.40$

Hammer 32.5H SA, 19200 lb-ft, Weight of ram = 3250 lb

Embedment, ft	10		55		110	
R_u, lb	10000		100000		200000	
% of R_u at tip	31		7.6		3.9	
Distance[a], ft	Tens.	Comp.	Tens.	Comp.	Tens.	Comp.
5	1142	2982	1006	2982	350	2956
10	2000	2966	1588	2966	718	2894
15	2478	2958	1889	2958	1120	2840
20	2642	2954	1868	2954	1434	2790
25	2566	2951	1765	2951	1541	2746
30	2571	2947	1798	2949	1584	2702
35	2575	2928	1814	2948	1668	2660
40	2630	2890	1798	2947	1739	2618
45	2463	2885	1582	2948	1567	2577
50	2432	2889	1593	2958	1621	2537
55	2544	2888	1634	2991	1839	2498
60	2622	2890	1821	2944	1899	2460
65	2205	2890	1447	2897	1468	2423
70	2004	2891	1352	2851	1390	2387
75	2477	2894	1719	2805	1850	2352
80	2561	2895	2014	2760	1958	2317
85	1812	2896	1318	2714	1182	2282
90	1241	2876	876	2649	791	2237
95	1932	2752	1482	2491	1636	2102
100	2147	2291	1895	2040	1836	1739
105	1454	1329	1281	1192	1149	1097
110	0	65	0	142	0	131
Permanent set of pile, in	2.77		0.61		0.27	

[a]From head of pile

increase was 90%.

Tables 7 and 8 show the same relationship between magnitude of tensile stresses and type of hammer.

The results of this section illustrate that tensile stresses during driving can be controlled by proper selection of the hammer and cushioning materials. The type of hammer is not of particular significance. The impact velocity of the ram is of overriding importance.

Port of San Francisco Case History

The 18-inch octagonal prestressed concrete piles were jetted to within three feet of penetration and then driven the final three feet (23). A double acting steam-air Vulcan 140C hammer with 36, 000 lb-ft of energy was used. The ram weight was 14, 000 lb. The cushion block was three inch thick Douglas-fir plywood. When driving with the hammer started, tension cracks appeared at about 12 inches on centers from the water line to top of pile. The cracks were noticed when puffs of dust occurred at each hammer blow. After several piles cracked and were replaced, jetting was eliminated. Occasional cracks still appeared. Finally the problem was solved by inserting 12 inches of cushion block and using a 20, 000 lb ram weight, while maintaining the 36, 000 lb-ft of energy.

In this study it was intended to determine whether the

cracking and no cracking situations could have been predicted. To complete information necessary to solve these problems, the weight of the pile cap was assumed to be 2, 000 lb; the capblock was assumed to be a Micarta (Nema grade C) which had a stiffness K_1=12, 000, 000 lb per inch. Its coefficient of restitution was 0.80. The stiffness for the three-inch thick Douglas-fir plywood was estimated from information provided by the Port of San Francisco. The skin friction was assumed to increase linearly with depth. The values of soil quake and damping for sands were assumed as suggested by Coyle (4). For the tip capacities of this case history the formula of bearing capacity for circular footings was used, although the actual cross section of the pile was an 18-inch octagon.

Since the pile was jetted through its tip into granular soil the percentage of ultimate soil resistance concentrated at the point was assumed to be zero. The ultimate soil resistance was then mainly due to the side friction. A friction angle of 30 degrees was assumed for the sand, the cohesion was assumed to be zero and the buoyant unit weight of the soil was 50 lb/ft^3. With this information the ultimate soil resistance was estimated from the static formulas, using the bearing capacity factors as given by Terzaghi (33).

Table 9. Maximum driving stresses in psi, along a 18" octagonal, 89' prestressed concrete pile, Port of San Francisco Case History.

$Q = 0.10$ in, $J = 0.15$ sec/ft, $J' = 0.00$ sec/ft

$K_1 = 12400000$ lb/in, $K_2 = 2740000$ lb/in

$e_1 = 0.80$, $e_2 = 0.52$

Energy of hammer = 36000 lb-ft, Weight of ram = 14000 lb

Embedment, ft	37		20		10	
R_u, lb	99000		62500		24000	
% of R_u at tip	0		54		70	
Distance[a], ft	Tens.	Comp.	Tens.	Comp.	Tens.	Comp.
5	1099	2739	1007	2739	1140	2739
10	1578	2735	1475	2735	1713	2735
15	1780	2736	1664	2736	1927	2736
20	1977	2740	1860	2740	2129	2740
25	1894	2746	1790	2746	2058	2745
30	1582	2743	1431	2743	1704	2739
35	1706	2677	1592	2677	1832	2671
40	1907	2602	1804	2591	2074	2586
45	1706	2631	1533	2630	1776	2625
50	1376	2786	1243	2782	1497	2777
55	1908	2796	1726	2791	1977	2785
62	1889	2794	1522	2800	1779	2794
69	1152	2778	808	2806	1073	2796
74	1387	2681	941	2742	1283	2730
79	1644	2272	1138	2377	1518	2366
84	1221	1343	761	1513	1000	1461
89	0	0	0	367	0	189
Permanent set of pile, in	3.34		2.29		3.12	

[a]From head of pile

Table 10. Maximum driving stresses in psi, along a 18" octagonal, 89' prestressed concrete pile, Port of San Francisco Case History.

$Q = 0.10$ in, $J = 0.15$ sec/ft, $J' = 0.00$ sec/ft

$K_1 = 12000000$ lb/in, $K_2 = 755000$ lb/in

$e_1 = 0.80$, $e_2 = 0.44$

Energy of hammer = 36000 lb-ft, Weight of ram = 20000 lb

Embedment, ft	20		10	
R_u, lb	62500		24000	
% of R_u at tip	54		70	
Distance[a], ft	Tens.	Comp.	Tens.	Comp.
5	411	1563	423	1558
10	593	1585	633	1579
15	605	1592	653	1591
20	461	1623	516	1622
25	294	1669	344	1667
30	392	1685	433	1684
35	441	1627	452	1623
40	271	1526	318	1516
45	112	1388	147	1383
50	329	1411	361	1405
55	349	1414	360	1407
62	237	1395	294	1385
69	40	1312	150	1295
74	188	1141	227	1126
79	171	895	237	891
84	18	663	173	544
89	0	270	0	140
Permanent set of pile, in	2.32		3.18	

[a]From head of pile

Tables 9 and 10 show the results for the problems outlined in Fig. 9. According to Table 9, when the 89 foot long pile is driven with a differential acting steam-air hammer Vulcan 140C and using the cushions indicated in the same table, the pile should have cracked whether it was embedded 10 feet, 20 feet or 37 feet, since the tensile stresses were considerably higher than the sum of the precompression stress and the ultimate tensile strength of the concrete. In the last case the jetting used to drive the pile 37 feet only adds to the problems, since no tip resistance will oppose the downward motion of the pile. The information from the field confirms that the pile suffered tensile cracking just after the driving was started.

Table 10 shows the maximum driving stresses and permanent set per blow when the weight of the ram was increased to 20, 000 lb and the thickness of the cushion had been increased to 12 inches. The maximum tensile stresses are less than the precompression stress, therefore, no cracking in the pile would be expected. The information from the field reveals that when these changes were made, tensile cracking of the piles did not develop.

Fig. 15 illustrates the situations of presence and absence of tension cracking in the pile. Both situations are for 10 feet of embedment. The cracking case corresponds to the lighter ram and

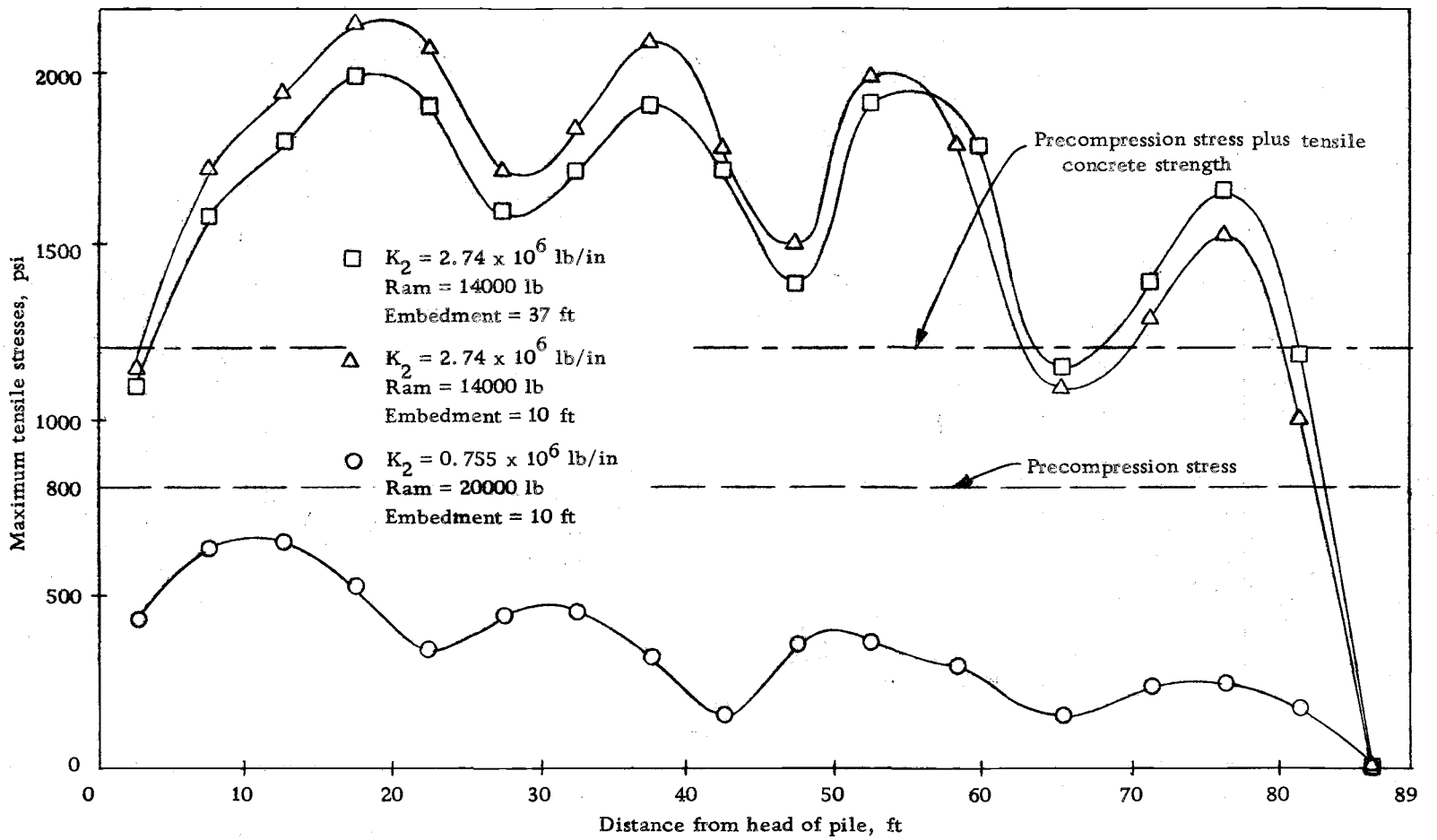

Figure 15. Maximum tensile stresses in an 89-foot prestressed concrete pile, Port of San Francisco Case History.

Table 11. Maximum driving stresses in psi, along a 18" octagonal, 89' prestressed concrete pile, Port of San Francisco Case History.

$Q = 0.10$ in, Emb. = 10 ft, $R_u = 24000$ lb, 70% at tip

$K_1 = 12000000$ lb/in, $K_2 = 755000$ lb/in

$e_1 = 0.80$, $e_2 = 0.44$

Energy of hammer = 36000 lb-ft, Weight of ram = 14000 lb

J, sec/ft	0.15		0.21		0.30	
J', sec/ft	0.05		0.07		0.10	
Distance[a], ft	Tens.	Comp.	Tens.	Comp.	Tens.	Comp.
5	537	1614	527	1614	512	1614
10	725	1630	709	1630	686	1630
15	724	1664	695	1664	659	1664
20	521	1699	509	1699	491	1699
25	419	1757	398	1757	360	1757
30	539	1767	514	1767	484	1768
35	559	1677	527	1678	483	1679
40	375	1552	335	1552	289	1552
45	414	1587	372	1587	320	1587
50	544	1612	509	1612	458	1613
55	500	1613	466	1614	416	1614
62	332	1589	288	1589	235	1590
69	547	1486	497	1487	432	1490
74	631	1289	582	1293	514	1297
79	499	1018	463	1023	410	1030
84	288	620	255	640	207	668
89	0	143	0	173	0	218
Permanent set of pile, in	3.03		2.91		2.78	

[a]From head of pile

Table 12. Maximum driving stresses in psi, along a 18" octagonal, 89' prestressed concrete pile, Port of San Francisco Case History.

$J = 0.15$ sec/ft, $J' = 0.05$ sec/ft

$K_1 = 12000000$ lb/in, $K_2 = 755000$ lb/in

$e_1 = 0.80$, $e_2 = 0.44$

Emb. = 10 ft, $R_u = 24000$ lb, 70% at tip

Energy of hammer = 36000 lb-ft, Weight of ram = 14000 lb

Q, in	0.10		0.15		0.20	
Distance[a], ft	Tens.	Comp	Tens.	Comp.	Tens.	Comp.
5	537	1614	537	1614	537	1614
10	725	1630	725	1630	725	1630
15	724	1664	724	1664	724	1664
20	521	1699	521	1699	521	1699
25	419	1757	419	1757	419	1757
30	539	1767	539	1767	539	1767
35	559	1677	559	1677	559	1677
40	375	1552	375	1552	375	1552
45	414	1587	414	1587	414	1587
50	544	1612	544	1612	544	1612
55	500	1613	500	1613	500	1613
62	332	1589	332	1589	332	1589
69	547	1486	547	1486	547	1486
74	631	1289	631	1289	631	1289
79	499	1018	499	1018	499	1018
84	288	620	288	620	288	620
89	0	143	0	143	0	143
Permanent set of pile, in	3.03		3.14		3.25	

[a]From head of pile

higher stiffness of cushion, while the no cracking case corresponds to the heavier ram and softer cushion.

Finally, Tables 11 and 12 show the results for the problems outlined in Figs. 10 and 11. Table 11 indicates that the higher the soil damping factors, the lower the tensile stresses and the permanent set of the pile per blow of hammer. Table 12 indicates that the variation of soil quake has no effect on the values of driving stresses. However, the permanent set of the pile increases as the quake increases. The fact that the driving stresses are not very sensitive to changes of the quake value was observed by Smith (32). This observation is significant since it permits the quake to be taken equal to 0.1 inches for most soils. Soil damping appears to be a significant factor and must be estimated with care.

The results presented for the San Francisco Case History indicate that for real situations, wave equation analysis is capable of predicting driving stresses with sufficient accuracy to forecast and solve tension cracking problems.

Oregon State Highway Division Test Pile

The test pile was a 12-inch square, 46-foot long prestressed concrete pile, it was driven with a differential acting steam-air Super Vulcan 65C hammer for the foundation of the Saint Louis

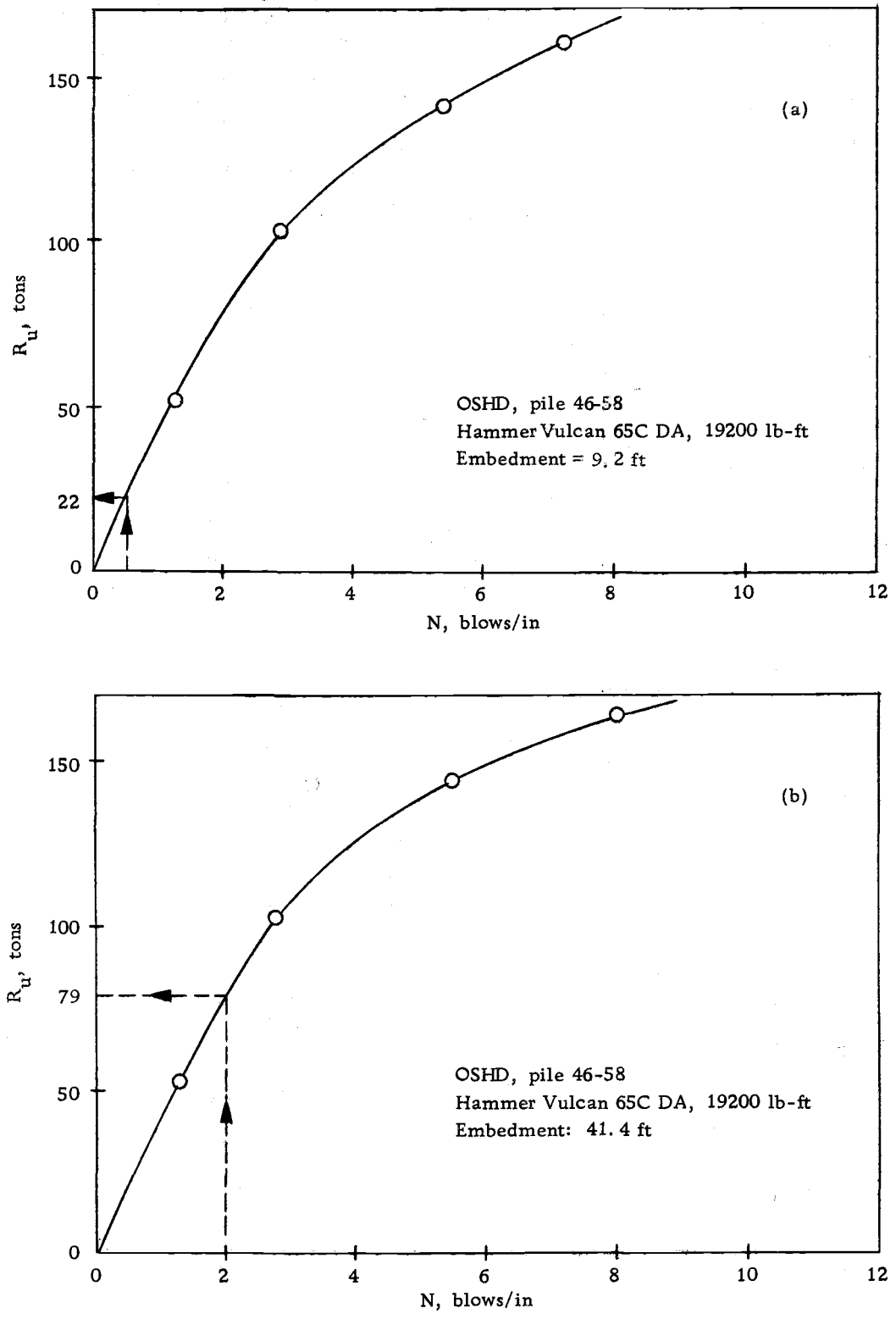

Figure 16. Ultimate soil resistances for Oregon State Highway Division Test Pile.

TEST PILE DRIVING RECORD

Bridge name St. Louis Rd. U-xing No. _____

Pile Location-Bent No. _____ Ftng. No. _____ Pile No. 46-58 Pile Type 12" x 12" Prest. Conc.

Resident Engineer _____ Inspector _____

Date 8/31/73 19 ____ Hammer Type Diff. Act. Steam-air Name Super Vulcan
Size 65C

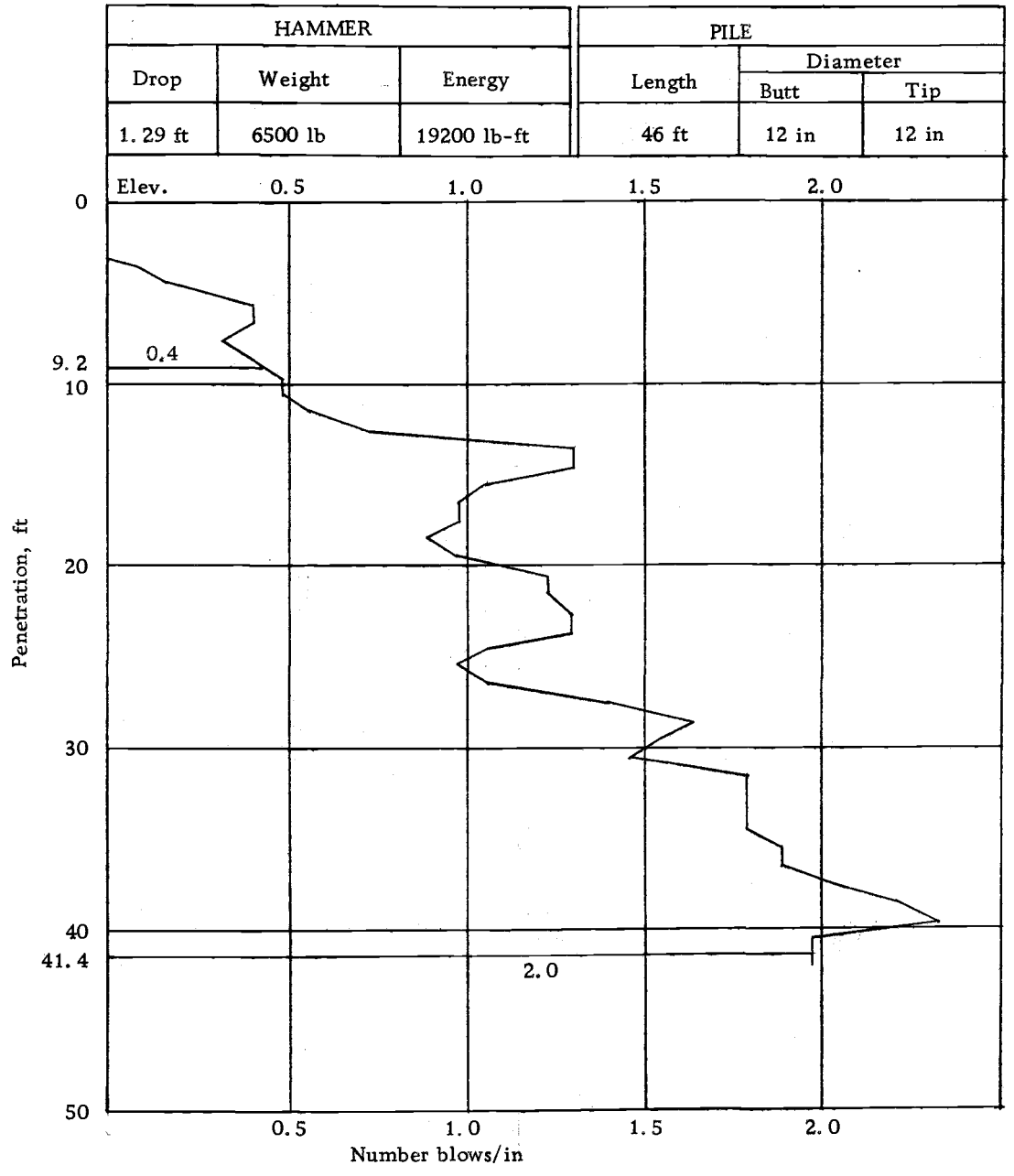

Figure 17. Driving record for Oregon State Highway Division Test Pile.

undercrossing bridge on Interstate 5, North of Salem. It was believed that high tensile stresses in the pile produced by the differential acting hammer could cause tensile cracking in the pile. This study was directed to determine whether such tension cracking was possible to predict under the circumstances which prevailed during driving.

The information available consisted of the driving record for the test pile shown in Fig. 17. In this particular case history the ultimate soil resistances were found from the wave equation solution (7) instead of computing them from static equations. Fig. 16 (a) and Fig. 16 (b) are such solutions and they were obtained with the same information used for the problems of Table 13. The driving record for the pile indicates that at 9.2 feet of embedment the number of blows per inch was 0.5, this value was entered into the curve of Fig. 16 (a) and the corresponding ultimate soil resistance was obtained. In similar way the ultimate soil resistance at 41.4 feet of embedment was determined using the 2.0 blows per inch of the driving record and entered into the curve of Fig. 16 (b). These two values of the ultimate soil resistances were used for the problems, the results of which are shown in Table 13.

In this instance, the main assumptions required were the values of soil parameters. For soft soils the value of quake Q was assumed to be 0.10 inches, point soil damping J equal to 0.15 seconds

Table 13. Maximum driving stresses in psi, along a 12" x 12" x 46' prestressed concrete pile, Oregon State Highway Division Test Pile.

$Q = 0.10$ in, $J = 0.15$ sec/ft, $J' = 0.05$ sec/ft

$K_1 = 1260000$ lb/in, $K_2 = 1150000$ lb/in

$e_1 = 0.40$, $e_2 = 0.40$

Energy of hammer = 19200 lb-ft

Embedment, ft	9.2				41.4			
R_u, lb	44000				158000			
% of R_u at tip	19.8				5.1			
Hammer type	65C DA		32.5H SA		65C DA		32.5H SA	
Distance[a], ft	Tens.	Comp.	Tens.	Comp.	Tens.	Comp.	Tens.	Comp.
4.6	442	2272	812	2623	304	2351	541	2708
9.2	610	2270	1364	2615	353	2269	977	2616
13.8	624	2270	1560	2611	567	2189	965	2528
18.4	577	2270	971	2611	649	2109	591	2442
23.0	186	2249	546	2608	528	2006	469	2353
27.6	293	2150	965	2552	430	1847	872	2215
32.2	517	1896	1290	2314	673	1565	1301	1935
36.8	639	1486	1479	1839	660	1150	1471	1453
41.4	459	824	1012	1203	469	626	1016	826
46.0	0	150	0	164	0	119	0	131
Permanent set of pile, in	1.80		1.37		0.47		0.31	

[a] From head of pile

per foot and side soil damping J' equal to 0.05 seconds per foot (4).

Table 13 shows that the maximum tensile stresses in the pile produced by driving with a differential acting hammer are less than the precompression stress of 800 psi. Therefore, the pile would not crack due to tensile stresses. The field information agrees with the above observation. The values of the compressive stresses shown in Table 13 are much lower than the ultimate compressive strength of the concrete. Therefore, no spalling of the concrete would be expected.

Fig. 18 is a plot of the tensile stresses shown in Table 13. The advantage of showing the results in this form is that the location of the cracking zone of the pile is immediately evident. According to these results, the pile would crack if it is driven with a single acting hammer of 19,200 lb-ft of energy and with a weight of ram of 3,250 lb.

Going back to Table 13, the permanent set of the pile per blow of double acting hammer is higher than its corresponding one for single acting hammer.

Tables 14 and 15 show the results for the problems outlined in Figure 13. The capblock was assumed to be a Micarta (Nema Grade C) with a coefficient of restitution e=0.80, and with a stiffness of 6,480,000 lb/in. The effect of these changes is to increase the driving stresses on the pile. Tables 14 and 15 also

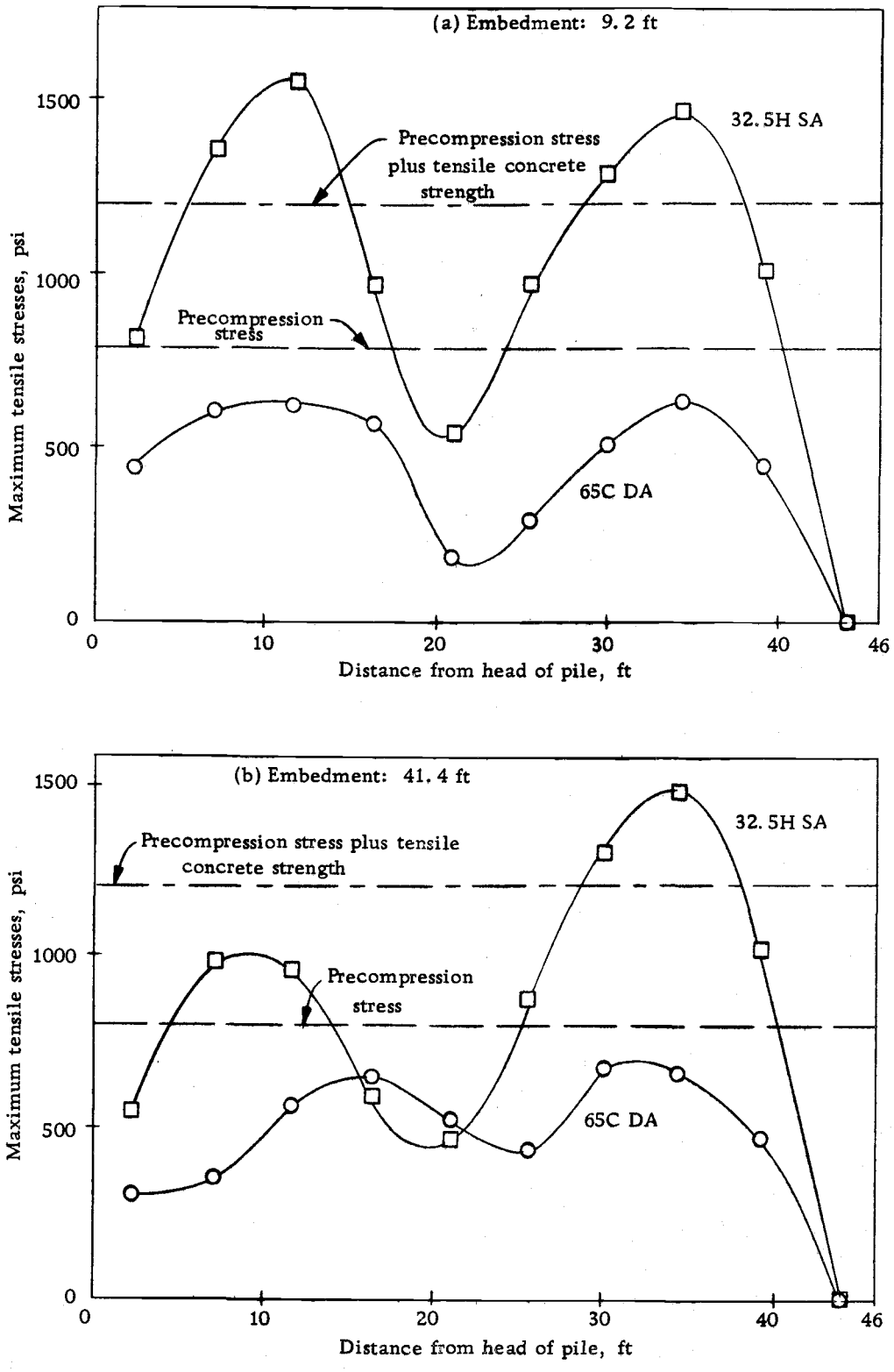

Figure 18. Maximum tensile stresses for Oregon State Highway Division Test Pile.

Table 14. Maximum driving stresses in psi, along a 12" x 12" x 46' prestressed concrete pile, Oregon State Highway Division Test Pile.

$Q = 0.10$ in, $J = 0.15$ sec/ft, $J' = 0.05$ sec/ft

$K_1 = 6480000$ lb/in, $K_2 = 1150000$ lb/in

$e_1 = 0.80$, $e_2 = 0.40$

Emb. = 9.2 ft, Hammer 65C DA, 19200 lb-ft

R_u, lb	10000		20000		30000		44000	
% of R_u at tip	19.8		19.8		19.8		19.8	
Distance,[a] ft	Tens.	Comp.	Tens.	Comp.	Tens.	Comp.	Tens.	Comp.
4.6	958	2515	874	2515	776	2515	744	2515
9.2	1286	2511	1089	2511	918	2511	842	2511
13.8	1186	2510	884	2510	773	2510	624	2510
18.4	1457	2510	1330	2510	1209	2510	1046	2510
23.0	1347	2510	1198	2510	1079	2510	916	2510
27.6	911	2505	638	2505	578	2506	486	2507
32.2	1083	2407	928	2410	815	2412	662	2416
36.8	1383	2033	1214	2048	1100	2060	944	2076
41.4	969	1209	896	1212	823	1217	725	1224
46.0	0	38	0	76	0	112	0	160
Permanent set of pile, in	3.62		2.70		2.19		1.75	

[a] From head of pile

Table 15. Maximum driving stresses in psi, along a 12" x 12" x 46' prestressed concrete pile, Oregon State Highway Division Test Pile.

$Q = 0.10$ in, $J = 0.15$ sec/ft, $J' = 0.05$ sec/ft

$K_1 = 6480000$ lb/in, $K_2 = 1150000$ lb/in

$e_1 = 0.80$, $e_2 = 0.40$

Emb. = 9.2 ft, Hammer 32.5H SA, 19200 lb-ft

R_u, lb	10000		20000		30000		44000	
% of R_u at tip	19.8		19.8		19.8		19.8	
Distance[a], ft	Tens.	Comp.	Tens.	Comp.	Tens.	Comp.	Tens.	Comp.
4.6	1204	3119	1151	3119	1116	3119	1066	3119
9.2	1765	3111	1598	3111	1481	3111	1322	3111
13.8	2381	3103	2230	3103	2101	3103	1925	3103
18.4	2485	3097	2350	3097	2214	3097	2030	3097
23.0	1849	3092	1663	3092	1545	3092	1384	3092
27.6	1797	3079	1375	3080	1175	3081	969	3082
32.2	2093	2977	1877	2981	1721	2985	1555	2991
36.8	2308	2534	2178	2547	2046	2558	1866	2573
41.4	1636	1511	1549	1514	1465	1522	1351	1532
46.0	0	44	0	87	0	129	0	184
Permanent set of pile, in	3.19		2.33		1.91		1.50	

[a]From head of pile

show that the higher the ultimate soil resistance, the lower the driving stresses will be. The permanent set of the pile per blow of hammer was higher for the double acting hammer than for the single acting hammer.

Table 14 shows that at 9.2 feet of embedment, the 46-foot pile driven by a full hammer blow with a Super Vulcan 65C will crack. To avoid this, the stiffness of the capblock may be modified by increasing its thickness or taking a softer material. This leads to the first case of Table 13.

In Table 15 the single acting hammer causes very high tensile stresses and cracking of the concrete would be immediate if necessary modifications would not be made. Such modifications might include changes of the cushion stiffnesses and some driving techniques. A half blow of the hammer would be helpful. Overall, the damaging effects of using the single acting hammer to drive the 46-foot pile of the example are very clear. The use of the double acting hammer would be more appropriate in this case.

The results presented for the Oregon State Highway Division Test Pile indicate that the wave equation analysis can be used to determine whether tension cracking problems can occur in a pre-stressed concrete pile driven with a certain type of hammer.

VII. SUMMARY AND CONCLUSIONS

On the basis of the hypothetical and case studies made, it is shown that potentially damaging effects on prestressed concrete piles are not exclusive with double acting steam-air hammers. Single acting hammers can also be harmful.

The behavior of a pile depends on the energy delivered by the hammer to the pile and the velocity of impact of the ram. The cushioning material and its thickness are important in the way the energy of the hammer is delivered to the pile. No absolute conclusions regarding the fitness of a pile hammer can be drawn for all cases of a given soil-pile system. A hammer that appears to be inadequate for a given situation, may perform satisfactorily by making some changes, such as decreasing the stiffness of the cushion or striking blows with a fraction of the full energy in the early stages of driving in soft soils.

Each individual situation can be considered using the methods of mechanics to select the best driving equipment. Discarding or accepting a given hammer on the basis of past experience alone is not necessary. The wave equation provides an efficient way to analyze potential choices.

When jetting is used to drive prestressed concrete piles, it is prudent to use reduced hammer energy until the driving

resistance increases. As the soil resistance increases, the energy of the hammer may be increased up to full capacity.

A double acting hammer that may be damaging to a given pile may not be harmful if some changes in the cushioning material and the driving practices are made.

The action designation of a hammer does not really describe the hammer in terms of how the pile-soil system responds to each blow. For example, as far as the driving stresses are concerned, it would make no difference whether 15, 000 lb-ft of energy is delivered by a single acting hammer Vulcan 1 or by a double acting hammer Vulcan 50C, because in both cases the velocity of impact at the head of the pile is practically the same.

Although several values of soil damping parameters have been suggested, more research in this respect is needed to obtain values for different types of soils that can be used in the wave equation, with more confidence. The value of 0.1 inch for the soil quake appears to be reasonable and changes from it have little influence on the magnitude of the driving stresses.

The value of the coefficient of restitution for the concrete to be used in the model needs more research. Since the stress-strain curve for the concrete is quite different from being linearly elastic, the coefficient of restitution may be different from 100%,

especially for higher values of stress on the concrete. Finally, an improvement on this method of analysis might be made by including the fatigue effects that successive blows of hammer on the pile may have, and hundreds of alterations in stresses that occur from one blow of the hammer.

BIBLIOGRAPHY

1. Bowles, Joseph E., Foundation Analysis and Design, McGraw-Hill Book Co., New York, 1968.

2. Brown, Thane E., "Handling and Driving Prestressed Concrete Piles." Presented at the 1962 Fall Meeting, American Concrete Institute, Seattle, September 1962.

3. Chellis, Robert, Pile Foundations, New York, McGraw-Hill, 1951, pp. 28-33, 449-450, 525-538.

4. Coyle, H.M., R.E. Bartoskewitz and K.W. Korb, "Soil Resistance Parameters for Wave Equation Analysis," Journal of Materials, JM LSA, Vol. 7, No. 4, December 1972, pp. 486-489.

5. Cummings, A. E., "Dynamic Pile Driving Analysis," Journal of the Boston Society of Civil Engineers, Jan. 1940, pp. 6-27.

6. Donnell, L.H., "Longitudinal Wave Transmission and Impact," ASME, Vol. 52, 1930, pp. 153-167.

7. Edwards, T.C., "Piling Analysis Wave Equation Computer Program Utilization Manual," Research Report Number 33-11 of the Texas Transportation Institute, Texas A&M University, College Station, Texas, August 1967.

8. Forehand, P. W. and J. L. Reese, "Pile Driving Analysis Using the Wave Equation," Master of Science in Engineering Thesis, Princeton University, 1963.

9. Forehand, P.W. and J.L. Reese, "Prediction of Pile Capacity by the Wave Equation," Journal of the Soil Mechanics and Foundation Division, ASCE, Vol. 90, No. SM2; Proc. Papers 3820, March 1964, p. 15.

10. Fox, E.N. "Stress Phenomena Occuring in Pile Driving," Engineering, (London) Vol. 134, pp. 216-263.

11. Gendron, G. J., "Pile driving: Hammers and Driving Methods," Highway Research Record, No. 33, 1970, pp. 16-22.

12. Gerwick, B. C., Jr., "Experience in the Use of Prestressed Concrete in Wharf & Harbor Construction," Off-print of the Papers of the 4th International Harbour Conference, Antwerp 22/27-6-1964.

13. Glanville, W. H., G. Grime, E. N. Fox and W. W. Davies, "An Investigation of the Stresses in Reinforced Concrete Piles During Driving," British Building Research Board Tech. Paper No. 20, D. S. I. R., 1938.

14. Hirsch, T. J., "Field Testing of Prestressed Concrete Piles During Driving," Report of the Texas Transportation Institute, Texas A & M University, August 1963.

15. Hirsch, T. J. and C. H. Samson, Jr., "Driving Practices for Prestressed Concrete Piles," Report of the Texas Transportation Institute, Texas A & M University, April, 1965.

16. Hirsch, T. J., "Fundamental Design and Driving Considerations for Concrete Piles," 45th Annual Meeting of Highway Research Board, Washington, D. C., January 1966.

17. Isaacs, D. V. "Reinforced Concrete Pile Formula," Institute of Australian Engineers Journal, Vol. 12, 1931, p. 312.

18. Lin, T. Y. and W. J. Talbot, "Pretensioned Concrete Piles Present knowledge summarized," Civil Engineering, May, May, 1961. p. 53.

19. Lin, T. Y. Design of Prestressed Concrete Structures, Second edition, John Wiley and Sons, Inc., New York, 1963.

20. Lowery, L. L., Jr., T. J. Hirsch and C. H. Samson, Jr., "Pile Driving Analysis - Simulation of Hammers, Cushions, Piles and Soil," Research Report 33-9 of the Texas Transportation Institute, Texas A & M University, College Station, Texas, August, 1967.

21. Oregon State Highway Division Personal Correspondence to W. L. Schroeder dated Nov. 2, 1973.

22. Oregon State Highway Commission, "Standard Specifications for Highway Construction," 1970, p. 269.

23. Peleaux, W. F., Personal Correspondence to W. L. Schroeder dated January 21, 1974.

24. Samson, C. H., Jr., T. S. Hirsch and L. L. Lowery, "Computer Study of Dynamic Behavior of Piling," Journal of the Structural Division, ASCE, Vol. 89 No. ST 4, Proc. Paper 3608, August, 1963.

25. Samson, C. H., Jr., F. C. Bundy and T. J. Hirsch, "Practical Applications of Stress-Wave Theory in Piling Design," presented to the annual Texas Section ASCE meeting, San Antonio, Texas, October, 1963.

26. Smith, E. A. L., "Pile Driving Impact," Proceedings, Industrial Computation Seminar, September, 1950, International Business Machines Corp., New York, N. Y., 1951, p. 44.

27. Smith, E. A. L. "Impact and Longitudinal Wave Transmission," Transactions, ASME, August, 1955, p. 963.

28. Smith, E. A. L. "What Happens When Hammer Hits Pile," Engineering News Record, McGraw-Hill Publishing Co., Inc., New York, N. Y., September 5, 1957, p. 46.

29. Smith, E. A. L., "The Wave Equation Applied to Pile Driving," Raymond Concrete Pile Co., 1957.

30. Smith, E. A. L., "Pile Calculations by the Wave Equation," Concrete and Constructional Engr., London, June 1958.

31. Smith, E. A. L., "Tension in Concrete Piles During Driving," Journal, Prestressed Concrete Institute, Vol. 5, 1960. pp. 35-40.

32. Smith, E. A. L., "Pile Driving Analysis by the Wave Equation," Journal of the Soil Mechanics and Foundation Division, ASCE, Vol. 86 No. SM4, August 1960, Part 1, pp. 35-61.

33. Terzaghi, Karl and Ralph B. Peck, Soil Mechanics in Engineering Practice, second edition, John Wiley & Sons, Inc., New York, 1948.

34. Timoshenko, S. P. and J. N. Goodier, Theory of Elasticity, 3rd ed., New York, McGraw-Hill, 1970.

APPENDIX

APPENDIX

NOTATION

A = cross sectional area, in square inches

B = damping constant for internal spring m, in seconds per foot

$C_{(m, t)}$ = compression of internal spring m in time interval t, in inches

c = velocity of propagation of stress wave, in inches per second

$D_{(m, t)}$ = displacement of external spring m in time interval t, in inches

$D'_{(m, t)}$ = plastic displacement of external spring m in time interval t, in inches

dx = infintesimal distance in x direction, in inches

E = modulus of elasticity, in pounds per square inch

$e_{(m)}$ = coefficient of restitution of internal spring m

$F_{(m, t)}$ = force in element m in time interval t, in pounds

g = acceleration due to gravity, in feet per second per second

$J_{(p)}$ = point soil damping constant, in seconds per foot

$J'_{(m)}$ = side soil damping constant at element m, in seconds per foot

$K_{(m)}$ = spring constant associated with internal spring m, in pounds per inch

$K'_{(m)}$ = spring constant of external spring m, in pounds per inch

K_s = spring constant to account for the dynamic application of load, in pounds per inch

m = element number

p = number of m at point pile

Q = quake or maximum ground deformation, in inches

$R_{(m, t)}$ = force exerted by external spring m on element m in time interval t, in pounds

$R_{u(m)}$ = ultimate ground resistance for external spring m, in pounds

$Slack_{(m)}$ = amount of movement required before $K_{(m)}$ will take tension, in inches

t = time for which calculations are being made

u = axial displacement of a bar cross section in x direction, in inches

$V_{(m, t)}$ = velocity of element m in time interval t, in feet per second

$W_{(m)}$ = weight of element m in pounds

x = direction of longitudinal axis of bar

ϵ = axial strain of a bar in x direction

ρ = mass per unit volume, in pounds second squared per inch to the fourth power

σ_x = axial stress in x direction, in pounds per square inch

Δt = size of time interval, in seconds

( ) = functional designation